

## Coversheet

# Experimental comparisons of carbonate-associated sulfate extraction methods

Zheyu Tian<sup>a</sup>, Graham A. Shields<sup>a</sup>, Ying Zhou<sup>a</sup>

<sup>a</sup>Department of Earth Sciences, University College London, WC1E 6BS, London, UK

Email Addresses: [z.tian.17@ucl.ac.uk](mailto:z.tian.17@ucl.ac.uk) (Zheyu Tian) [g.shields@ucl.ac.uk](mailto:g.shields@ucl.ac.uk) (Graham Shields) [y-zhou@ucl.ac.uk](mailto:y-zhou@ucl.ac.uk) (Ying Zhou)

This manuscript has been submitted for publication in *Chemical Geology*. Please note that this paper is a non-peer reviewed EarthArXiv preprint. Subsequent versions of this manuscript may have slightly different content. If accepted, the final version of this manuscript will be available via the "Peer-reviewed Publication DOI" link on the right-hand side of this webpage. Please feel free to contact any of the authors; we welcome feedback.

# 1 Experimental comparisons of carbonate-associated sulfate extraction methods

2 Zheyu Tian<sup>a</sup>, Graham A. Shields<sup>a</sup>, Ying Zhou<sup>a</sup>

3 <sup>a</sup>Department of Earth Sciences, University College London, WC1E 6BS, London, UK, [z.tian.17@ucl.ac.uk](mailto:z.tian.17@ucl.ac.uk)

## 4 5 1 Abstract

6  
7 Carbonate-associated sulfate (CAS) refers to trace amounts of sulfate incorporated into carbonate  
8 minerals during precipitation. CAS has been the most commonly used approach to recover the paleo-  
9 seawater sulfate sulfur isotope composition ( $\delta^{34}\text{S}_{\text{sw}}$ ) as carbonate rocks are more common and occur in  
10 less restricted marine environments than alternative sulfate-bearing minerals (such as gypsum and  
11 anhydrite). However, uncertainties remain about the reliability of preparation techniques due to the  
12 inadvertent inclusion of contaminant sulfurous species. This study applied three oxidative leaching CAS  
13 extraction methods and compared their final  $\delta^{34}\text{S}_{\text{CAS}}$  values with those following repeated single leaching  
14 in 10% NaCl (aq). The final  $\delta^{34}\text{S}_{\text{CAS}}$  values after sequential leaching by a combined 12% NaOCl, 1% H<sub>2</sub>O<sub>2</sub>,  
15 and 10% NaCl approach were systematically higher by between 0.65‰ and 0.90‰ than rival methods.  
16 Our experiments indicate that contamination can affect measured  $\delta^{34}\text{S}_{\text{CAS}}$  even given short reaction times  
17 (<30 min). A single leach with standard oxidizing reagents may not entirely eliminate contamination when  
18 handling organic and pyrite-rich carbonate samples.

19 **Keywords:** Carbonate-associated sulfate; CAS extraction; Contaminant sulfur; Sulfur isotopes

## 20 21 2 Introduction

22  
23 Carbonate-associated sulfate (CAS) refers to trace sulfate that was incorporated into carbonate  
24 minerals during precipitation (Burdett et al., 1989). CAS has been used as a reliable proxy archive for  
25 tracing paleo-seawater isotopic composition since the 1980s (Burdett et al., 1989; Staudt and Schoonen,  
26 1995; Kampschulte and Strauss, 2004; Bottrell and Newton, 2006; Tostevin et al., 2017). Compared with  
27 sulfate minerals (barite and sulfate evaporite minerals), which generally precipitate from derived seawater,  
28 CAS co-precipitates with normal marine carbonate minerals and so  $\delta^{34}\text{S}_{\text{CAS}}$  can serve as a more reliable  
29 tracer of the isotopic evolution of seawater sulfate ( $\delta^{34}\text{S}_{\text{SW}}$ ) and may even be used for chemostratigraphic  
30 correlation (Kampschulte and Strauss, 1998; Tostevin et al., 2017; Shi et al., 2018; Edwards et al., 2019;  
31 He et al., 2019). Moreover, carbonate deposits occur more widely and in less restricted marine  
32 environments than other sulfate minerals, further underlining the potential of CAS to better understand the  
33 long-term global sulfur cycle (Marenco et al., 2008b).

34 Despite such promise,  $\delta^{34}\text{S}_{\text{CAS}}$  might still deviate from  $\delta^{34}\text{S}_{\text{SW}}$  due to post-depositional alteration  
35 during meteoric water-rock interaction and recrystallization (Present et al., 2015). Such issues can  
36 generally be resolved after careful petrological (crystal size, mineral assemblages) and geochemical  
37 screening. For example, recrystallized carbonate crystals are usually larger (>50 $\mu\text{m}$ ) with lower  $\delta^{18}\text{O}$   
38 values (Al-Aasm and Clarke, 2004; Zhang et al., 2020) and higher Mn/Sr ratios (Kaufman and Knoll,  
39 1995; Bartley et al., 1998; Lan et al., 2019). Cross-plots of  $\delta^{34}\text{S}_{\text{CAS}}$  against traditional indicators of  
40 diagenetic alteration, CAS concentration, Mn/Sr, Mg/Ca and  $\delta^{18}\text{O}_{\text{carb}}$  values are therefore widely used to  
41 evaluate carbonate diagenesis and the fidelity of measured  $\delta^{34}\text{S}_{\text{CAS}}$  values (Veizer, 1983; Derry et al., 1994;  
42 Goldberg et al., 2005; Guo et al., 2015; He et al., 2019). Nevertheless, it seems unlikely that such alteration  
43 proxies can reliably identify deviation from open ocean  $\delta^{34}\text{S}_{\text{SW}}$  values due to mineral precipitation from  
44 porewaters affected by early diagenetic microbial sulfate reduction (MSR) (Rennie and Turchyn, 2014;  
45 Fike et al., 2015). MSR results in <sup>34</sup>S-enrichment in the residual sulfate reservoir, while sulfide oxidation

46 may conversely release  $^{34}\text{S}$ -depleted sulfate into porewaters. Although these effects are difficult to assess  
47 in individual samples and may lead to uncertainty over the contemporaneous  $\delta^{34}\text{S}_{\text{SW}}$  value, systematic  
48 trends and similar correlative  $\delta^{34}\text{S}_{\text{CAS}}$  values are unlikely to result from such localized isotopic  
49 fractionation.

50 The thorniest problem surrounding  $\delta^{34}\text{S}_{\text{CAS}}$  studies pertains to the inadvertent extraction of sulfate  
51 from the non-carbonate matrix of bulk carbonate rocks, including secondary atmospheric sulfate (SAS),  
52 organic-bound sulfur (OSC), disseminated pyrite (Py), and other metastable metal-sulfide minerals, with  
53  $\delta^{34}\text{S}$  values down to -50‰ (Canfield, 2001; Sim et al., 2011; Hoefs, 2015). It has been demonstrated, in  
54 particular, that pyrite oxidation can occur in both strong and weak acids during the CAS extraction process  
55 (Marenco et al., 2008b). Such non-CAS sulfate sources may contaminate extracted CAS, resulting in  
56 lowered  $\delta^{34}\text{S}_{\text{CAS}}$  values (Lomans et al., 2002; Marenco et al., 2008a; Peng et al., 2014). The extent of  
57 deviation from primary values is dependent not only on the amount and isotopic composition of the  
58 contaminants but also on the chosen analytical protocols (Wotte et al., 2012; Fichtner et al., 2017). Even  
59 working with well-preserved carbonate samples, generating a reliable CAS signal without incorporating  
60 non-CAS contaminants is still a key consideration when using the CAS approach.

61 In order to produce reliable CAS signals, two different approaches have been proposed for CAS  
62 extraction. The first of these techniques (Aim-I) aims to eliminate soluble salts and SAS, as well as hinder  
63 further pyrite oxidation by washing samples in 10% NaCl solution before final extraction. It was first used  
64 to isolate structurally substituted sulfate from both sedimentary carbonate and phosphate minerals  
65 (Kampschulte and Strauss, 1998; Shields et al., 1999; Kampschulte et al., 2001). A slightly different  
66 method was developed by (Shen et al., 2008; Li et al., 2010; Shen et al., 2011), who washed their samples  
67 firstly with 10% NaCl for 24 h and then washed them three times with deionized water. Wotte et al. (2011,  
68 2012) washed their samples with 10% NaCl until no leachable sulfate was precipitated, following addition  
69 of barium chloride. A five times 10% NaCl wash in between washing with deionized water three times  
70 has been widely used in recent years (Tostevin et al., 2017; He et al., 2019; Ma et al., 2021). The second  
71 approach (Aim-II) aims to eliminate organic sulfur and disseminated pyrite by adding oxidants such as  
72 NaOCl or  $\text{H}_2\text{O}_2$  (Burdett et al., 1989; Hurtgen et al., 2002; Marenco et al., 2008a; Guo et al., 2015). Various  
73 comparative experimental studies have been carried out. One slight difference between these methods is  
74 the leaching sequence using those solutions. For example, Burdett et al. (1989) soaked the samples with  
75 5.25% NaOCl before the final CAS extraction step. Gellatly and Lyons (2005) rinsed their samples with  
76 deionized water before adding the 5.25% NaOCl. Gill et al. (2007) added two more deionized water rinse  
77 steps after washing with 4% NaOCl. Loyd et al. (2012b) washed samples four times with deionized water  
78 before the NaOCl wash, although they consider their data to have been affected by pyrite oxidation. In  
79 contrast to Loyd et al. (2012b), Thompson and Kah (2012) switched the order of deionized water and  
80 NaOCl washes.

81 Other Aim-I trials to prevent sulfide oxidation have included using  $\text{N}_2$  carrier gas under anaerobic  
82 conditions to prevent the oxidation of acid volatile sulfides and pyrite (Newton et al., 2004; Bottrell and  
83 Newton, 2006; Wei et al., 2020). Other Aim-II trials to use oxidants to remove reduced sulfur included  
84 adding 30%  $\text{H}_2\text{O}_2$  for 48 h to 30-100g sample powder before or after rinsing with 10% NaCl solution and  
85 deionized water (Shen et al., 2011; Xiao et al., 2012) and roasting the samples at 600°C for 4 h after a 10%  
86 NaCl wash with a subsequent deionized water rinse to isolate phosphate-bound sulfate (Goldberg et al.,  
87 2011). Highly concentrated 30%  $\text{H}_2\text{O}_2$  (aq) is not stable (might cause spontaneous combustion when in  
88 contact with organic material) and will cause partial dissolution of the carbonate portions as  $\text{H}_2\text{O}_2$  (aq) is  
89 also a weak dibasic acid. Nevertheless, the addition of salt rinses, after deliberate oxidation, has the

90 potential to guarantee the effective removal of both oxidized sulfide and the remaining oxidizing reagent.

91 Many of these CAS extraction techniques are very similar. Wotte et al. (2012) compared a range of  
92 pre-leaching techniques: Aim-I: 1) 10% NaCl (aq); 2) pure water only (aq); and Aim-II: 1) 10% NaOCl  
93 (aq) only; 2) 10% NaCl (aq) followed by 10% NaOCl (aq); 3) 10% NaCl (aq) followed by 10% H<sub>2</sub>O<sub>2</sub> (aq).  
94 The authors noted that pre-leaching with those oxidizing agents was insufficient to remove all non-CAS  
95 contamination from even finely ground, bulk carbonate rock powder, while residual oxidants proved  
96 difficult to eradicate fully. As a consequence, they recommended a single reagent NaCl pre-leaching  
97 method (Aim-I), commenting further that the addition of oxidizing agents (NaOCl and H<sub>2</sub>O<sub>2</sub>) as the last  
98 pre-leaching step could potentially oxidize surviving sulfide minerals in the residue, thus contaminating  
99 the extracted CAS sulfate. However, for organic and pyrite-rich carbonate samples, this simplified method  
100 might still incorporate contaminant sulfur due to oxidation during the experiment.

101 In this study, we designed and compared three CAS extraction methods in order to eliminate all non-  
102 CAS sulfur-bearing phases using oxidizing agents (Aim-II) for bulk carbonate rock CAS extraction. Pure  
103 reagents need to be used so as not to add contaminant ions, while methods need to ensure that oxidants  
104 are completely removed in the final CAS extraction steps. The three methods are: (1) 10% H<sub>2</sub>O<sub>2</sub> (aq)  
105 followed by 10% NaCl (aq); (2) 12% NaOCl (aq) followed by 10% NaCl (aq); (3) Combined NaOCl then  
106 H<sub>2</sub>O<sub>2</sub> followed by 10% NaCl (aq). We compared these three oxidative leaching methods against a refined  
107 single reagent 10% NaCl (aq) leaching method (He et al., 2019) in order to identify contaminant sulfur  
108 sources and their influence on the measured CAS sulfur isotope values. Here we present the results of  
109 those experiments in order to establish a more effective CAS extraction protocol for dealing with  
110 problematic organic and/or pyrite-rich carbonate rocks.

### 112 **3 Sample selection, pre-treatment, and analytical methodology**

114 We first extracted CAS using a single 10% NaCl method (method 1) for around 80 carbonate samples  
115 during the Ediacaran Period in South China and then selected four representative samples to test the  
116 oxidative methods. Basic descriptions of the selected samples are given in Table 1, while more detailed  
117 descriptions can be found in the Supplementary Materials. The samples were selected based on three  
118 criteria: 1) the most common carbonate rock types; 2) a wide range of CAS concentrations and  $\delta^{34}\text{S}_{\text{CAS}}$   
119 values; 3) a wide range of pyrite and TOC contents.

120 Hand specimens of these samples were first cleaned with water and cut into small blocks in order to  
121 remove weathered surfaces before being heated in an oven at 60°C for 48 hours to dry them out thoroughly.  
122 One of the dried blocks was used for making thin sections at University College London (UCL) and  
123 studied petrographically. The other blocks were first broken into small pieces, and only the pieces without  
124 veins were chosen to be grounded into powder in a tungsten carbide Tema mill and crushed again by hand  
125 with an agate mortar to maximize its surface area and expose interstitial pyrite. After the crushing process,  
126 the machine was cleaned carefully with DI water and acetone to prevent contamination between samples.

127 For the elemental test, including Ca, Mg, Mn, Sr, Al, K, Fe concentrations, around 20mg of carbonate  
128 rock powder was dissolved in 10ml 2% HNO<sub>3</sub> overnight and centrifuged before being analyzed using a  
129 *Varian*® 720 ICP-OES at the London Geochemistry and Isotope Centre (LOGIC) at UCL. The Laboratory  
130 control solution standard samples were tested after every 20 samples to monitor the drift and precision.  
131 The analytical precision for all elemental analyses was better than 5% (1SD).

132 Pyrite density was estimated using a petrographic microscope at UCL. Pyrite crystals were counted  
133 within a 1×1 mm<sup>2</sup> area. For each sample, five representative 1×1 mm<sup>2</sup> areas were chosen to estimate the

134 pyrite density of the sample. The pyrite crystal sizes are relatively homogeneous and range from 7-16 $\mu$ m  
 135 (See supplementary). The final qualitative pyrite density reflects the average number of pyrite crystals  
 136 within a 1 $\times$ 1 mm<sup>2</sup> area in each thin section. Samples with pyrite density < 10/mm<sup>2</sup> were labelled as low  
 137 pyrite density, 10/mm<sup>2</sup> < pyrite density < 100/mm<sup>2</sup> labelled as medium pyrite density, and pyrite density >  
 138 100/mm<sup>2</sup> labelled as high pyrite density.

139 Solid inorganic sulfides, operationally defined as acid volatile sulfur (AVS) and chromium reducible  
 140 sulfur (CRS), were extracted in the Geobiology Laboratory at the University of St Andrews using the  
 141 chromium reduction method, as previously described (Canfield et al., 1986; Zerkle et al., 2012; Izon et al.,  
 142 2015). Briefly, 5-10 g of rock powder was placed in a tri-neck flask and sequentially refluxed with 6M  
 143 HCl to release AVS, followed by acidified 1M CrCl<sub>2</sub> to release CRS. The resulting H<sub>2</sub>S gas was carried  
 144 on a stream of oxygen-free N<sub>2</sub> into a solution of AgNO<sub>3</sub> and captured as silver sulfide (Ag<sub>2</sub>S) for sulfur  
 145 isotope analyses.

146 We used deionized water and sulfate-free reagents for cleaning and oxidative leaching in this study  
 147 (see Method X). The detail of the CAS extraction procedures will be discussed later. After CAS extraction,  
 148 sulfate was collected as barium sulfate using excess BaCl<sub>2</sub> (aq). The BaSO<sub>4</sub> from CAS extraction and Ag<sub>2</sub>S  
 149 from AVS, CRS extraction were weighed into tin cups plus vanadium pentoxide catalyst and combusted  
 150 at 1,080°C to yield SO<sub>2</sub> for sulfur isotope analysis by EA-IRMS (ANCA-GSL/20-20; SerCon®, Crewe,  
 151 UK) on dried residues of > 0.05mg at the Iso-Analytical Ltd. Laboratory, UK. The reference material used  
 152 for analysis was IA-R061 (barium sulfate,  $\delta^{34}\text{S}_{\text{CDT}} = +20.33\text{‰}$ ). IA-R025 (barium sulfate,  $\delta^{34}\text{S}_{\text{V-CDT}} =$   
 153  $+8.53\text{‰}$ ), IA-R026 (silver sulfide,  $\delta^{34}\text{S}_{\text{V-CDT}} = +3.96\text{‰}$ ) and IAEA-SO-5 (barium sulfate,  $\delta^{34}\text{S}_{\text{V-CDT}} =$   
 154  $+0.5\text{‰}$ ). S isotope values are reported in the  $\delta$  notation against V-CDT. We also obtained %S data from  
 155 the total ion beam data recorded by the mass spectrometer, which was then used to calculate the purity of  
 156 the precipitates. Duplicate samples and reference samples (IA-R061 and IAEA-SO-5) were measured  
 157 every five samples for quality control. Analytical precision was better than 0.06‰ (1SD).

158 Total organic carbon (TOC) content was analyzed using a *Leco*® *CS-200* carbon analyzer at UCL.  
 159 About 1g of sample powders was weighed and reacted with excess 10% HCl to eliminate carbonate,  
 160 followed by repeated rinsing with Milli-Q water to remove contamination. The residual was dried at 40°C  
 161 for 48 hours for the TOC test. Analytical precisions within 1% (1SD).

162  
 163  
 164

Table 1: Selected late Ediacaran carbonate samples from South China (QLKS = Qinglinkou section, CC = Zhimaping section, LH = Lianghong section). Pyrite density: Low < 10/mm<sup>2</sup>; Medium 10-100/mm<sup>2</sup>; High >100/mm<sup>2</sup>.

Sample	Geological unit	Lithology	CaCO <sub>3</sub> (wt%)	[CAS] (ppm)	Pyrite Density	$\delta^{34}\text{S}_{\text{CAS}}$ (‰) NaCl rinse
QLKS18	Upper Shibantan Member, Dengying Formation	Grey fine-grained dolomitic limestone rock with white calcite veins	50.36	21.73	3.70/mm <sup>2</sup> Low	35.84
QLKS6	Middle Shibantan Member, Dengying Formation	Dark grey thinly laminated micritic limestone rock with white calcite veins	91.63	27.29	22.50/mm <sup>2</sup> Medium	46.00
CC3	Lower Shibantan Member, Dengying Formation	Dark thin banded micritic limestone rock rich in organic matter.	76.63	111.53	236.10/mm <sup>2</sup> High	36.52
LHA6.5	Member III, Doushantuo Formation	Grey fine-grained banded limestone	84.92	78.84	17.90/mm <sup>2</sup> Medium	20.21

#### 165 4 Refined NaCl leaching method (method 1)

166  
167 Many previous studies used large amounts (30-250g or even larger) of samples for CAS extraction  
168 (Wotte et al., 2012; Xiao et al., 2012; Shi et al., 2018; Toyama et al., 2020). However, using smaller and  
169 more finely ground samples can significantly decrease the risk of contamination by non-CAS components  
170 in bulk carbonate powders, especially for deep-time CAS studies. Moreover, incomplete leaching due to  
171 large sample sizes can mean that measured CAS values might not represent the whole rock CAS signals.  
172 In these regards, the NaCl leaching method (Kampschulte and Strauss, 1998; Wotte et al., 2011; Wotte et  
173 al., 2012) (see Fig. 1-A) has been applied increasingly to smaller samples (~10g) for pre-Cambrian and  
174 Cambrian studies (Tostevin et al., 2017; He et al., 2019). In this study, we tested around 80 samples before  
175 comparing methods and found that 8-10g samples are large enough in this case to extract sufficient CAS  
176 for isotopic analysis.

177 It has been shown by (He et al., 2019; He et al., 2020) that the sulfur concentration in the NaCl-  
178 leachates declines dramatically through sequential leaching, reaching near blank levels after the third or  
179 fourth leach for most carbonate samples. In our study, rock powder was leached therefore five times in an  
180 actively mixed 10% NaCl solution over 24 hours, followed each time by centrifugation to remove the  
181 supernatant. Between each leach, the residue was washed three times with deionized water. After the final  
182 leach with NaCl solution, the residue was washed five times with deionized water, followed by immediate  
183 CAS extraction using 6 M HCl (aq).

184 After the pre-leaching, we used excess acid (6M HCl) for the final dissolution step (8-10g samples)  
185 for all tested CAS extraction methods (Fig. 1-D). Reaction time was kept to no more than 30 minutes to  
186 minimize the potential of pyrite oxidation (He et al., 2019). The solution was then filtered using a  
187 polyethylene syringe and a 0.2 $\mu$ m polypropylene membrane filter (Wynn et al., 2008). Some previous  
188 studies used saturated BaCl<sub>2</sub> solution (358g/L, 20°C, ~26.4%) to precipitate barium sulfate at room  
189 temperature (Wynn et al., 2008; Li et al., 2017; Tostevin et al., 2017; Edwards et al., 2019; He et al., 2019).  
190 Some others used 12% BaCl<sub>2</sub> (Wotte et al., 2011; Wotte et al., 2012), 10% BaCl<sub>2</sub> (Markovic et al., 2016),  
191 or 8.5% BaCl<sub>2</sub> (Theiling and Coleman, 2015) to precipitate sulfate. However, adding saturated BaCl<sub>2</sub> (aq)  
192 into the decarbonated HCl solution may cause BaCl<sub>2</sub> to precipitate instead of BaSO<sub>4</sub>, thus removing Ba<sup>2+</sup>  
193 ions from the solution that might have reacted with SO<sub>4</sub><sup>2-</sup>. After several tests, we found that adding 1.5 ml  
194 200g/L BaCl<sub>2</sub> (aq) improved the purity of the yield (Fig. 1-D). Another option for future studies could be  
195 to use sulfate-free barium iodide or barium nitrate.

196 In this study, 1.5 ml 200g/L (~16.7%) BaCl<sub>2</sub> (aq) was added to the filtrate. Once sealed, sample tubes  
197 were left at room temperature for 3-4 days in order to precipitate released trace sulfate as barium sulfate.  
198 After centrifugation and supernatant removal, the residue was rinsed with 6M HCl and deionized water to  
199 remove any remaining acid-soluble components, such as BaCl<sub>2</sub> and BaCO<sub>3</sub>, and dried at 60°C for three  
200 days. Finally, precipitates were collected in a tin capsule for  $\delta^{34}\text{S}$  analysis on EA-IRMS. Although we  
201 washed the precipitates beforehand, some samples were still not pure barium sulfate (possibly containing  
202 residual BaCl<sub>2</sub> or H<sub>2</sub>O). We back-calculated the BaSO<sub>4</sub> yield based on the %S data.

203 This method is easy to handle and can remove most water-soluble sulfate and SAS in the carbonate  
204 powder. However, the method does not seek to eliminate AVS, CRS, and organic sulfur, which could  
205 undergo partial oxidation during CAS extraction. Therefore, this method could potentially generate a  
206 different, most likely lower  $\delta^{34}\text{S}_{\text{CAS}}$  value compared with the actual carbonate value, which should  
207 approximate the  $\delta^{34}\text{S}_{\text{sw}}$  value of contemporaneous seawater.

208

## 209 5 Three oxidative leaching methods

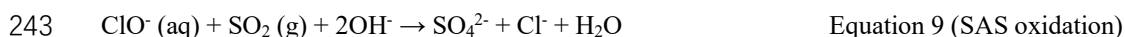
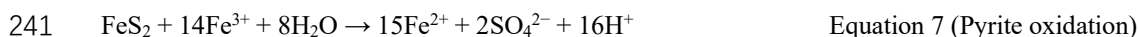
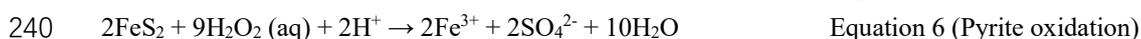
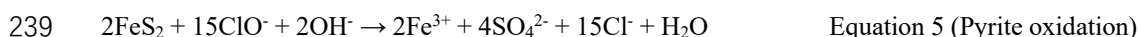
### 210 5.1 H<sub>2</sub>O<sub>2</sub> and NaOCl leaching (methods 2a and 2b)

211

212 These two methods were developed from a combined NaCl-NaOCl leach method, as applied by (Gill  
213 et al., 2011a; Gill et al., 2011b), in which 10% NaCl solution is first added to the samples for 24h.  
214 Subsequently, 5-10 g of the carbonate powders are washed twice with deionized water and then soaked in  
215 4% NaOCl solution for 48h in order to oxidize the non-CAS sulfur. Two additional washes with deionized  
216 H<sub>2</sub>O follow this step. Wotte et al. (2012) argued that this method has the following drawbacks: 1) It cannot  
217 ensure the elimination of pyrite; and 2) It cannot totally remove the oxidants before CAS extraction.  
218 Consequently, if the powder is not sufficiently fine, interstitial pyrite might be oxidized in the subsequent  
219 CAS extraction process by a combination of Fe (III) and any oxidants that remain in the slurry (Equation  
220 5-8).

221 In our revised single oxidative methods (Fig. 1-B), samples were leached firstly with 10% H<sub>2</sub>O<sub>2</sub> (aq)  
222 solution (method 2a) or 12% NaOCl (aq) solution (method 2b) for 24 h in order to remove the SAS  
223 (Equation 9, 10), organic sulfur and pyrite (Equations 5-8). As NaOCl (aq) and H<sub>2</sub>O<sub>2</sub> (aq) are not stable at  
224 high concentrations, we chose a relatively stable concentration for this study. All the anticipated reactions  
225 in the slurry are shown in Equations 1-10. These oxidants have been widely used by, for example  
226 (Ohkouchi et al., 1999; Hurtgen et al., 2002; Newton et al., 2004; Shen et al., 2011; Loyd et al., 2012a;  
227 Xiao et al., 2012). The leaching procedure was repeated three times for 24h each. In order to disintegrate  
228 the powder further, remove the calcium sulfate coating on pyrite crystal surface (Brunner, 2003) and  
229 maximize pyrite surface area, an ultrasonic bath was used between vigorous shaking using a rotator. The  
230 residue was washed three times with deionized water between each leach to remove the oxidized sulfur in  
231 the slurry. Nearly no barium sulfate precipitate was observed after the third leach, after which the residue  
232 was washed repeatedly using the refined 10% NaCl (aq) leaching method (Fig. 1-A) to remove the  
233 remaining sulfate, SAS, and remaining oxidant in the slurry.

234



245

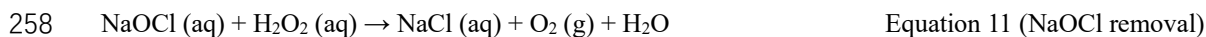
### 246 5.2 Combined NaOCl-H<sub>2</sub>O<sub>2</sub> leaching (method 3)

247

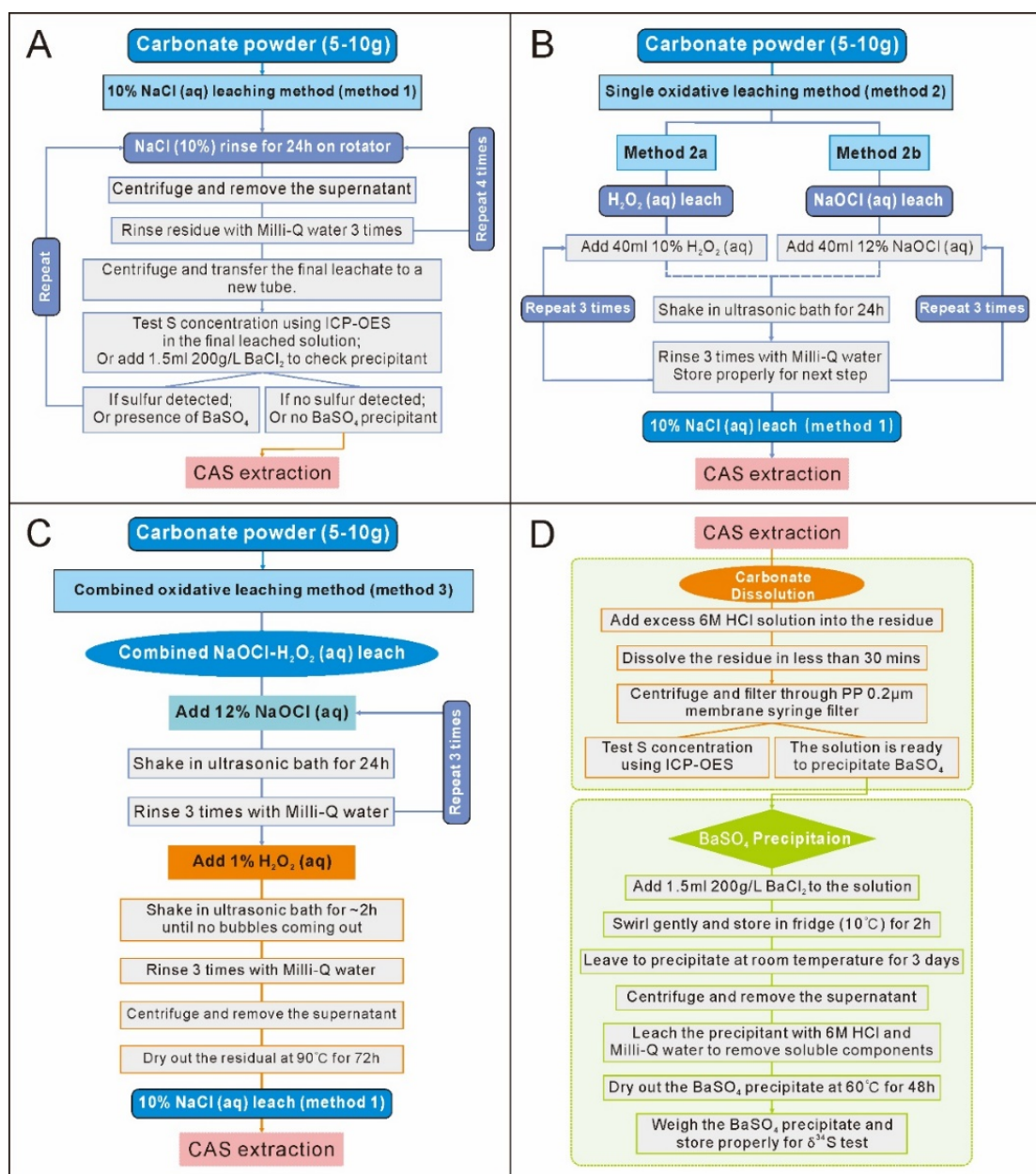
248 According to the study by (Wotte et al., 2012), it is hard to completely eliminate oxidants in the slurry.  
249 The new combined oxidative leaching method (method 3) in this study was designed to solve this issue  
250 (Fig. 1-C). After final leaching with NaOCl and Milli-Q water in method 2b, 1% H<sub>2</sub>O<sub>2</sub> (aq) was added to  
251 the slurry in order to remove the NaOCl (Equation 11). Using only 1% H<sub>2</sub>O<sub>2</sub> (aq) could minimize the  
252 potential for dissolution of our carbonate samples as H<sub>2</sub>O<sub>2</sub> is a weak acid. The absence of bubbles shows

253 whether the NaOCl was successfully removed from the slurry. Moreover, the addition of hydrogen  
 254 peroxide will not add further contaminant ions to the slurry, while being unstable, it can be easily removed  
 255 by heating at 90°C (Equation 12), followed by the refined 10% NaCl (aq) leaching method, as shown in  
 256 Fig. 1-A.

257



260



261

262 Fig. 1. New designed and tested carbonate-associated sulfate (CAS) pre-leaching and extraction protocols in this study.

263 A: Refined 10% NaCl (aq) pre-leaching method (method 1). B: Single oxidative-NaCl pre-leaching methods: 10% H<sub>2</sub>O<sub>2</sub> (aq) leach

264 (method 2a) and 12% NaOCl leach (aq) (method 2b). C: Combined NaOCl-H<sub>2</sub>O<sub>2</sub>-NaCl pre-leaching method (method 3). D:

265 Refined CAS extraction protocols.

266 **6 Results**

267

268 Leachate precipitate weights, sulfur isotope values, and final CAS sulfur isotope values are shown in  
 269 Table 2. Because precipitates are rarely pure barium sulfate, we back-calculated barium sulfate weights  
 270 based on the purity data obtained during isotopic analysis. The leachate precipitate sulfur isotope values  
 271 are shown as  $\delta^{34}\text{S}_{\text{SL}}$ , and the final CAS sulfur isotope values are shown as  $\delta^{34}\text{S}_{\text{CAS}}$ . For method 2a, as  $\text{H}_2\text{O}_2$   
 272 (aq) is a weak dibasic acid, it will cause partial dissolution of samples. Moreover,  $\text{H}_2\text{O}_2$  (aq) is not stable  
 273 and might cause spontaneous combustion at concentrations higher than 8% in contact with organic  
 274 material, so we have not tested the leachate sulfur isotope value of all samples using method 2a. As  
 275 QLKS18 is a dolostone sample with a low sulfate concentration (Table 1), we failed to get the final CAS  
 276 sulfur isotope data. All the elemental test data are shown in the Supplementary Information (Table S1).  
 277 Sample LHA6.5 is a pure limestone with very low pyrite and TOC content, so we did not obtain AVS and  
 278 CRS sulfur isotope values from this sample.

279

280 Table 2. Leachate precipitate weight, sulfur isotope composition, and final CAS sulfur isotope values from different pre-leaching  
 281 methods together with the TOC content, AVS, CRS concentration, and its sulfur isotope values of the samples.

282 “--” means too low to get a reliable value. SL = solution. S isotope values are reported in the  $\delta$  notation against V-CDT.

Sample	Method	Powder weight (g)	Rinse Times	BaSO <sub>4</sub> Corrected (mg)	Leachate $\delta^{34}\text{S}_{\text{SL}}$ (‰)	CAS $\delta^{34}\text{S}_{\text{CAS}}$ (‰)	Method 1 $\delta^{34}\text{S}_{\text{CAS}}$ (‰)	AVS		CRS		TOC (wt%)
								S (ppm)	$\delta^{34}\text{S}_{\text{AVS}}$ (‰)	S (ppm)	$\delta^{34}\text{S}_{\text{CRS}}$ (‰)	
QLKS18	2a	7.59	1	1.39			35.84	4.00	--	9.75	30.47	0.022
			2	1.84	--	--						
			3	1.09								
	2b	8	1	0.08	20.65							
			2	0.63	--	--						
			3	0.33	--							
3	8	4	0.12	--	--							
QLKS6	2a	7.5	1	0.34		46.00	1.41	--	90.50	37.16	0.14	
			2	0.77	--							--
			3	0.17								
	2b	8	1	0.12	31.82							
			2	0.15	20.28							46.37
			3	0.05	--							
3	8	4	0.03	--	46.79							
CC3	2a	7.52	1	133.37		36.52	16.05	24.26	1769.16	22.19	2.53	
			2	2.42	--							--
			3	0.16								
	2b	8	1	134.24	24.15							
			2	0.84	20.45							36.91
			3	0.04	18.88							
3	8	4	0.04	--	37.42							
LHA6.5	2a	7.51	1	0.13		20.21	1.37	--	13.77	--	0.013	
			2	1.09	--							--
			3	0.29								
	2b	8	1	0.08								
			2	0.33	--							20.72
			3	0.11								
3	8	4	0.08	--	20.86							

283

## 284 7 Discussion

### 285 7.1 Evaluation of the three oxidative leaching methods

286

287 NaOCl leachates with a pink to brown color show how after adding oxidants to the slurry, iron (likely  
288 in the form of pyrite) and possibly TOC, have been oxidized (supplementary Fig. S1). Fig. 2-A, B shows  
289 that the final barite precipitate (back-calculated) weight from the leached solutions using all these three  
290 tested methods shows a similar trend towards zero after the third leach. Only sample CC3, which is dark  
291 limestone with the highest pyrite density and TOC content, shows a continuously decreasing trend of the  
292 precipitate weight (grey line). The other samples show that the second leachate has the most sulfate. The  
293 third and fourth leachates have similar precipitate weights almost below the lower limit for S isotope  
294 analysis (Fig. 2-C), which confirms that nearly all the contaminant S has been removed by leach steps 3  
295 or 4.

296 All leachates have significantly lower sulfur isotope  $\delta^{34}\text{S}_{\text{SL}}$  values compared with the final  $\delta^{34}\text{S}_{\text{CAS}}$   
297 values (~ 13-26‰ lower) (Table 2), indicating that the leaching process removes contaminant sulfur-  
298 bearing species (atmospheric sulfate or SAS, organic sulfur, and pyrite) rather than CAS. The first  
299 leachates from samples QLKS18, QLKS6, and CC3, all from the Shibantan Member of the Dengying  
300 Formation, have the highest sulfur isotope values with  $\delta^{34}\text{S}_{\text{SL}}$  of 20.65‰, 31.82‰, and 24.15‰  
301 respectively, whereas second and third leachates of those samples have consistent  $\delta^{34}\text{S}_{\text{SL}}$  values around  
302 20‰.

303 Fig. 2-D shows the final  $\delta^{34}\text{S}_{\text{CAS}}$  value using the different methods. Compared with a single reagent  
304 10% NaCl (aq) pre-leaching method, our methods 2b and 3 show incrementally higher final  $\delta^{34}\text{S}_{\text{CAS}}$  values  
305 for the same sample. For samples QLKS6, CC3, and LHA6.5, there is a systematic difference of 0.79‰,  
306 0.90‰, and 0.65‰, respectively, between the NaCl leaching method and the combined oxidative method  
307 3. These relative differences (see Fig. 2-E) mirror the samples' visually estimated pyrite density (17.9,  
308 22.5, and 236.1) and measured AVS + CRS contents, respectively (Table 2). Our experiment reveals  
309 method 3 to be the favoured method in the sense that it will more likely result in pristine CAS sulfur  
310 isotope values for pyrite-rich samples. Although systematic in direction, the differences are relatively  
311 minor, due perhaps in part to the high  $\delta^{34}\text{S}_{\text{SL}}$ ,  $\delta^{34}\text{S}_{\text{CRS}}$ , and  $\delta^{34}\text{S}_{\text{AVS}}$  values, relative to  $\delta^{34}\text{S}_{\text{CAS}}$ .

312

### 313 7.2 Contaminant sulfur evaluation

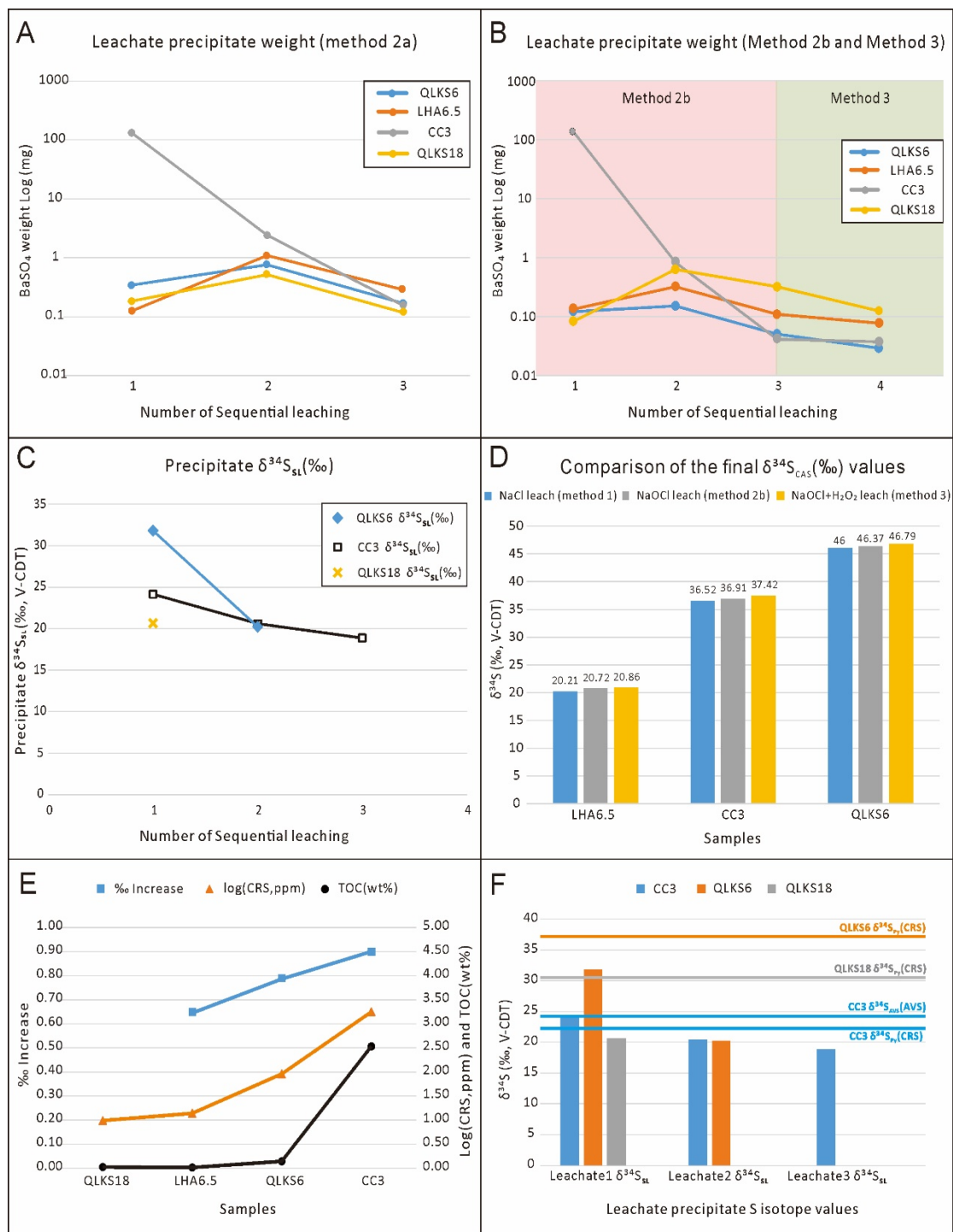
314

315 Atmospheric  $\text{SO}_2$  can potentially influence final CAS sulfur isotope values but is relatively hard to  
316 evaluate (Peng et al., 2014). Moreover, SAS sulfur is likely to be sorbed onto the surfaces of carbonate  
317 crystals (Edwards et al., 2019) and so ought to be leached out with repeated rinsing with 10% NaCl (aq).  
318 In this study, therefore, we mainly tested the S isotope values of AVS and CRS (pyrite) in each sample and  
319 the TOC content in order to evaluate the potential influence of other sulfur-bearing contaminants on our  
320 final CAS sulfur isotope values. Sample CC3, which has the highest pyrite and TOC content, exhibits the  
321 greatest difference between CAS sulfur isotope values. Although LHA6.5 and QLKS6 have similar TOC  
322 contents, sample QLKS6, which has a higher CRS concentration, shows a greater change in the final CAS  
323 value. Our results confirm therefore that TOC content and/or pyrite content can significantly influence  
324 measured  $\delta^{34}\text{S}_{\text{CAS}}$  values (Fig. 2-E).

325 Fig. 2-F shows that except for sample CC3, leachate  $\delta^{34}\text{S}_{\text{SL}}$  values are lower than  $\delta^{34}\text{S}_{\text{CRS}}$ . As pyrite  
326 sulfur and organic sulfur compounds (OSC) are the two main sulfur sources in TOC-rich carbonate  
327 samples (Werne et al., 2003), we consider therefore that OSC might lower the leachate sulfur isotope

328 values. The origin and composition of the organic sulfur compounds are still not fully understood, but it  
329 has been reported that organic sulfur isotope values are at least 8‰ lower than ambient seawater sulfate  
330 (Siedenberg et al., 2018), while kerogen sulfur was reported to range widely between -32.6‰ and 30.3‰  
331 in Archean stromatolite samples (Bontognali et al., 2012). The first leachate precipitate weight of sample  
332 CC3 is around 100 times higher than the highest values from the other samples, even though its AVS +  
333 CRS concentration is only 20 times higher, indicating perhaps that the difference between  $\delta^{34}\text{S}_{\text{SL}}$  and  
334  $\delta^{34}\text{S}_{\text{CRS}}$  values was caused by oxidizing other sulfur sources, possibly the OSC.

335 We note that  $\delta^{34}\text{S}_{\text{SL}}$  values show a decreasing trend and that leachates 2 and 3 have relatively stable  
336 isotope values of around 20‰. It seems that the first leachate is more complex, whereby the first leachate  
337 of sample CC3 has nearly the same sulfur isotope value as AVS: 24.15‰ and 24.26‰, respectively. As  
338 SAS is unlikely to influence leachate sulfur isotope values, the first leachate seems more likely to represent  
339 a combination of both AVS and CRS. However, leachate 2, and especially leachate 3 might be more  
340 influenced by the oxidation of organic sulfur.



341  
 342  
 343  
 344  
 345  
 346  
 347  
 348  
 349  
 350

Fig. 2. Comparison and evaluation of four methods result in this study. A: Barite precipitate weight from 3 leachates using method 2a. B: Barite precipitate weight from 3-4 leachates using method 2b (shaded in pink) and 3 (shaded in green). C: Leachate sulfate sulfur isotope values  $\delta^{34}S_{st}$ . D: Comparison of the final CAS sulfur isotope value  $\delta^{34}S_{CAS}$  using three different methods (NaCl only, methods 2b, and method 3). E: Comparison between the gradient of CAS  $\delta^{34}S_{CAS}$  increase from NaCl pre-leaching to method 3 and samples' CRS concentration and TOC content (The % increase refers to the increase in the  $\delta^{34}S_{CAS}$  values from method 1 to method 3). F: Comparison of the leachate precipitate S isotope value with pyrite S isotope value showing the leachate S isotope values are consistently lower than the coeval pyrite S isotope values. Sample CC3 (dark limestone with the highest pyrite density and AVS + CRS concentration) has the highest % increase of the final  $\delta^{34}S_{CAS}$  value, then QLKS6 (dark grey limestone), then LHA6.5 (grey limestone).

### 7.3 Comparisons with published CAS data

This study investigated the sulfur isotope systematics of three carbonate samples from the Shibantan Member, Dengying Formation (CC3, QLKS6, QLKS18), and one sample from Doushantuo Member III (LHA6.5) (supplementary Fig. S2). In the Yangtze Gorges area, the Dengying Formation is subdivided into three members, which from bottom to top are the siliceous dolostone Hamajing Member, dark banded limestone Shibantan Member, and light grey dolostone Baimatuo Member. These three members can be correlated with the Algal Dolomite Member, Gaojiashan Member, and Beiwan Member, respectively, in the southern Shaanxi Gaojiashan area (Chen et al., 2015; Cui et al., 2016). At the Gaojiashan section, CAS sulfur isotope values do not change much (average  $42.40 \pm 3.74\%$ ). Further afield, the Dengying Formation is often correlated with the late Ediacaran Nama Group in Namibia (Tostevin et al., 2017). For sample LHA6.5, with the carbon isotope value  $-8.1\%$  (Lu et al., 2013), it can be correlated with relatively stable values ( $-8.9\%$ ) from the upper Doushantuo member III ( $\sim 120\text{--}140$  m) at the Jiulongwan section (Shi et al., 2018).

The CAS sulfur isotope data and  $\Delta\delta^{34}\text{S}$  data from this study and published equivalent samples' data are summarized in Table 3. Our average  $\delta^{34}\text{S}_{\text{CAS}}$  using method 3 is  $40.02\%$ , which is comparable with stratigraphically equivalent samples from the Gaojiashan Member, Gaojiashan section ( $42.40\%$ ) (Cui et al., 2016) but higher than values from the Gaojiashan Member, Lianghekou section ( $36.1\%$ ) (Chen et al., 2015) and the correlative Nama group ( $34.13\%$ ) (Tostevin et al., 2017). Although we only tested three samples from the Shibantan Member for this study, one sample yielded a  $\delta^{34}\text{S}_{\text{CAS}}$  value of  $46.8\%$ , which is higher than all published values from either the Gaojiashan Member or the Nama Group. Our results suggest that the improved method 3 here could significantly prevent the inclusion of contaminant sulfur (up to  $15.2\%$  lower than resultant CAS, Table 2) and generate more reliable  $\delta^{34}\text{S}_{\text{CAS}}$  values. Moreover, by oxidizing the contaminant sulfur, our new method 3 could prevent the incorporation of contaminant O from water  $\text{H}_2\text{O}$  or dissolved oxygen  $\text{O}_2$  (Equation 7, 8), which could potentially generate more reliable CAS  $\delta^{18}\text{O}_{\text{CAS}}$  too.

In summary, our experiments outlined here demonstrate that method 3 is a potentially superior method for handling organic-rich (high TOC content) and pyrite-rich limestone samples. However, if the sample is pure limestone with low pyrite density and TOC content, repeated pre-leaching with  $10\%$  NaCl is still shown to be both straightforward and relatively reliable.

### 7.4 Rethinking the 'Superheavy Pyrite'

The phenomenon of high sulfide sulfur isotope values (higher than contemporaneous sulfate sulfur isotope values) has been referred to as the 'superheavy pyrite' problem (Ries et al., 2009). However, sedimentary pyrite sulfur  $\delta^{34}\text{S}_{\text{PY}}$  can seldom if ever be isotopically heavier than its ambient sulfate reservoir  $\delta^{34}\text{S}_{\text{sulfate}}$ , which has puzzled geochemists for decades (Canfield, 2001; Fike et al., 2015; Cui et al., 2018). Superheavy pyrite has been reported from Neoproterozoic successions around the world, but in particular from the late Ediacaran Nama Group (Ries et al., 2009). Data from Tostevin et al. (2017) indicate, however, a much smaller  $\Delta\delta^{34}\text{S}_{\text{CAS-PY}}$  in those same successions of only less than  $1\%$  ( $-0.72 \pm 5.68\%$ , Table 3, supplementary Fig. S3), with only two samples having higher pyrite sulfur  $\delta^{34}\text{S}_{\text{PY}}$  than  $\delta^{34}\text{S}_{\text{CAS}}$ . In this regard, it may be significant that  $\delta^{34}\text{S}_{\text{CRS}}$  values from our study, although high, up to  $37.2\%$ , are consistently lower than  $\delta^{34}\text{S}_{\text{CAS}}$  values from the same sample. It may still be argued therefore that 'superheavy pyrite' might just be 'heavy pyrite', which can be achieved in a low sulfate environment via

395 Rayleigh distillation (Chen et al., 2008; Ries et al., 2009; Wood et al., 2015). Cui et al. (2018) proposed  
 396 that post-depositional TSR might generate high pyrite sulfur  $\delta^{34}\text{S}_{\text{PY}}$ . However, hydrothermal activity is a  
 397 local process, and not all isotopically heavy pyrite has been subject to hydrothermal influence (Wang et  
 398 al., 2019). Moreover, isotopically heavy pyrite might also form in shallow, high sedimentation rate  
 399 environments, which involves partial oxidation of the sulfide during frequent sedimentary reworking (Fike  
 400 et al., 2015). Until more reliable isotopic data come out, the origins or even existence of ‘superheavy pyrite’  
 401 (see also Wang et al., 2019) will likely remain obscure.

402 Table 3. Comparisons between CAS sulfur isotope values  $\delta^{34}\text{S}_{\text{CAS}}$  and  $\Delta\delta^{34}\text{S}_{\text{CAS-PY}}$  from this study and published data. ‘n’ indicates  
 403 the sample number. Errors are one standard deviation.

Lithostratigraphy	Samples	$\delta^{34}\text{S}_{\text{CAS}}$ highest	$\delta^{34}\text{S}_{\text{CAS}}$ lowest	$\delta^{34}\text{S}_{\text{CAS}}$ mean	$\Delta\delta^{34}\text{S}_{\text{CAS-PY}}$
Middle Dengying Formation (~550-546 Ma)	This study Shibantan member Qinglinkou section (Method 3)	46.79‰	35.84‰	40.02 ± 5.92‰ (n=3)	10.08 ± 4.95‰ (n=3)
	Cui et al. (2016) Gaojiashan member Gaojiashan section	45.8‰	32.5‰	42.4 ± 3.7‰ (n=42)	34.7 ± 9.6‰ (n=26)
	Chen et al. (2015) Gaojiashan member Lianghekou section	37.8‰	33.1‰	36.1 ± 2.2‰ (n=4)	--
	Tostevin et al. (2017) Nama Group Namibia	45.43‰	21.87‰	34.13 ± 5.34‰ (n=51)	-0.72 ± 5.68‰ (n=11)
Doushantuo Member III (~570-551 Ma)	This study Upper Doushantuo Lianghong section (Method 3)	20.86‰	20.86‰	20.86‰	--
	McFadden et al. (2008) Upper Doushantuo Jiulongwan section	43.5‰	6.9‰	20.7 ± 8.6‰ (n=50)	22.8 ± 10.0‰ (n=18)
	Shi et al. (2018) Upper Doushantuo Jiulongwan section	34.3‰	13.5‰	20.2 ± 6.3‰ (n=14)	24.8 ± 11.8‰ (n=13)

404

## 405 8 Conclusions

406

407 In this study, we designed and compared three oxidative CAS leaching methods with the refined  
 408 NaCl leaching method in order to establish a robust protocol for bulk carbonate rock CAS extraction. Our  
 409 experiments demonstrate that:

- 410 (1) The combined oxidizing method ‘12% NaOCl + 1% H<sub>2</sub>O<sub>2</sub> followed by repeated 10% NaCl  
 411 leaching’ is, by comparison, the most suitable method to handle samples with high pyrite and  
 412 organic contents. If the sample is pure limestone with low pyrite density, repeated pre-leaching  
 413 with 10% NaCl is more straightforward and relatively reliable.

- 414 (2) Our new method 3 could prevent the incorporation of contaminant O from the water H<sub>2</sub>O and/or  
415 dissolved oxygen O<sub>2</sub>, which could potentially generate more reliable CAS  $\delta^{18}\text{O}_{\text{CAS}}$ .
- 416 (3) The final CAS sulfur isotope values ( $\delta^{34}\text{S}_{\text{CAS}}$ ) using the combined 12% NaOCl + 1% H<sub>2</sub>O<sub>2</sub>  
417 method were between 0.65‰ and 0.9‰ higher than rival methods.
- 418 (4) Even with short reaction times (<30 min) to extract CAS, non-CAS contaminants (organic sulfur,  
419 and especially pyrite sulfur) still have the potential to lower final CAS sulfur isotope  
420 compositions  $\delta^{34}\text{S}_{\text{CAS}}$ .
- 421 (5) Our experiment confirms that a single leaching step with oxidizing reagents is commonly not  
422 enough to remove all contaminant sulfate.
- 423 (6) By adding oxidizing agents NaOCl and H<sub>2</sub>O<sub>2</sub>, we successfully oxidized pyrite and OSC. The  
424 first leachate likely represents a combination of both AVS and CRS. However, leachates 2 and 3  
425 are more likely to represent the organic sulfur isotope values  $\delta^{34}\text{S}_{\text{OSC}}$ .
- 426 (7) Our study suggests that organic sulfur isotope values  $\delta^{34}\text{S}_{\text{OSC}}$  can be significantly different from,  
427 and in this case, lower than the coeval pyrite sulfur isotope value  $\delta^{34}\text{S}_{\text{PY}}$ .
- 428 (8) Our data fit well with published data from South China and Namibia but show consistently high  
429  $\delta^{34}\text{S}_{\text{CAS}}$  values.
- 430 (9) With only ~0.7‰ difference between CAS sulfur and pyrite sulfur isotope values  $\Delta\delta^{34}\text{S}_{\text{CAS-PY}}$  in  
431 published ‘superheavy pyrite’ studies, it is worthwhile to revisit such cases with improved CAS  
432 extraction methods in future studies.

433

#### 434 **Acknowledgments**

435

436 ZHEYU TIAN is supported by a co-funded UCL-CSC research scholarship. This work was supported  
437 by the co-funded UK-China NERC-NSFC BETR Program NE/P013643/1. We thank Dr. Aubrey Zerkle  
438 for helping extract inorganic sulfides at the University of St Andrews. We also thank Dr. Tianchen He  
439 (Leeds) and Dr. Wei Shi (CUG Wuhan) for giving helpful suggestions and Gary Tarbuck for technical  
440 support.

## References

- Al-Aasm, I.S., Clarke, J.D., 2004. The effect of hydrothermal fluid flow on early diagenetic dolomitization: an example from the Devonian Slave Point Formation, northwest Alberta, Canada.
- Bartley, J.K., Pope, M., Knoll, A.H., Semikhatov, M.A., Petrov, P., 1998. A Vendian-Cambrian boundary succession from the northwestern margin of the Siberian Platform: stratigraphy, palaeontology, chemostratigraphy and correlation. *Geol Mag*, 135(4): 473-94.
- Bontognali, T.R. et al., 2012. Sulfur isotopes of organic matter preserved in 3.45-billion-year-old stromatolites reveal microbial metabolism. *Proc Natl Acad Sci U S A*, 109(38): 15146-51.
- Bottrell, S.H., Newton, R.J., 2006. Reconstruction of changes in global sulfur cycling from marine sulfate isotopes. *Earth-Science Reviews*, 75(1-4): 59-83.
- Brunner, B., 2003. *The Sulfur cycle: From bacterial microenvironment to global biogeochemical cycles*, ETH Zurich.
- Burdett, J.W., Arthur, M.A., Richardson, M., 1989. A Neogene Seawater Sulfur Isotope Age Curve from Calcareous Pelagic Microfossils. *Earth and Planetary Science Letters*, 94(3-4): 189-198.
- Canfield, D.E., 2001. Biogeochemistry of Sulfur Isotopes. *Reviews in Mineralogy and Geochemistry*, 43(1): 607-636.
- Canfield, D.E., Raiswell, R., Westrich, J.T., Reaves, C.M., Berner, R.A., 1986. The use of chromium reduction in the analysis of reduced inorganic sulfur in sediments and shales. *Chemical geology*, 54(1-2): 149-155.
- Chen, X., Li, D., Ling, H.-F., Jiang, S.-Y., 2008. Carbon and sulfur isotopic compositions of basal Datangpo Formation, northeastern Guizhou, South China: Implications for depositional environment. *Progress in Natural Science*, 18(4): 421-429.
- Chen, Y., Chu, X., Zhang, X., Zhai, M., 2015. Carbon isotopes, sulfur isotopes, and trace elements of the dolomites from the Dengying Formation in Zhenba area, southern Shaanxi: Implications for shallow water redox conditions during the terminal Ediacaran. *Science China Earth Sciences*, 58(7): 1107-1122.
- Cui, H. et al., 2016. Environmental context for the terminal Ediacaran biomineralization of animals. *Geobiology*, 14(4): 344-63.
- Cui, H. et al., 2018. Questioning the biogenicity of Neoproterozoic superheavy pyrite by SIMS. *American Mineralogist*, 103(9): 1362-1400.
- Derry, L., Brasier, M., Corfield, R.e.a., Rozanov, A.Y., Zhuravlev, A.Y., 1994. Sr and C isotopes in Lower Cambrian carbonates from the Siberian craton: a paleoenvironmental record during the 'Cambrian explosion'. *Earth and Planetary Science Letters*, 128(3-4): 671-681.
- Edwards, C.T., Fike, D.A., Saltzman, M.R., 2019. Testing carbonate-associated sulfate (CAS) extraction methods for sulfur isotope stratigraphy: A case study of a Lower–Middle Ordovician carbonate succession, Shingle Pass, Nevada, USA. *Chemical Geology*, 529.
- Fichtner, V. et al., 2017. Diagenesis of carbonate associated sulfate. *Chemical Geology*, 463: 61-75.
- Fike, D.A., Bradley, A.S., Rose, C.V., 2015. Rethinking the Ancient Sulfur Cycle. *Annual Review of Earth and Planetary Sciences*, 43(1): 593-622.
- Gellatly, A.M., Lyons, T.W., 2005. Trace sulfate in mid-Proterozoic carbonates and the sulfur isotope record of biospheric evolution. *Geochimica et Cosmochimica Acta*, 69(15): 3813-3829.
- Gill, B.C., Lyons, T.W., Jenkyns, H.C., 2011a. A global perturbation to the sulfur cycle during the

- Toarcian Oceanic Anoxic Event. *Earth and Planetary Science Letters*, 312(3-4): 484-496.
- Gill, B.C., Lyons, T.W., Saltzman, M.R., 2007. Parallel, high-resolution carbon and sulfur isotope records of the evolving Paleozoic marine sulfur reservoir. *Palaeogeography, Palaeoclimatology, Palaeoecology*, 256(3-4): 156-173.
- Gill, B.C. et al., 2011b. Geochemical evidence for widespread euxinia in the later Cambrian ocean. *Nature*, 469(7328): 80-3.
- Goldberg, T., Poulton, S.W., Strauss, H., 2005. Sulphur and oxygen isotope signatures of late Neoproterozoic to early Cambrian sulphate, Yangtze Platform, China: diagenetic constraints and seawater evolution. *Precambrian Research*, 137(3-4): 223-241.
- Goldberg, T., Shields, G.A., Newton, R.J., 2011. Analytical Constraints on the Measurement of the Sulfur Isotopic Composition and Concentration of Trace Sulfate in Phosphorites: Implications for Sulfur Isotope Studies of Carbonate and Phosphate Rocks. *Geostandards and Geoanalytical Research*, 35(2): 161-174.
- Guo, H. et al., 2015. Sulfur isotope composition of carbonate-associated sulfate from the Mesoproterozoic Jixian Group, North China: Implications for the marine sulfur cycle. *Precambrian Research*, 266: 319-336.
- He, T. et al., 2020. An enormous sulfur isotope excursion indicates marine anoxia during the end-Triassic mass extinction. *Sci Adv*, 6(37): eabb6704.
- He, T. et al., 2019. Possible links between extreme oxygen perturbations and the Cambrian radiation of animals. *Nat Geosci*, 12(6): 468-474.
- Hoefs, J., 2015. *Stable Isotope Geochemistry*. Springer.
- Hurtgen, M.T., Arthur, M.A., Suits, N.S., Kaufman, A.J., 2002. The sulfur isotopic composition of Neoproterozoic seawater sulfate: implications for a snowball Earth? *Earth and Planetary Science Letters*, 203(1): 413-429(1): 413-429.
- Izon, G. et al., 2015. Multiple oscillations in Neoarchaean atmospheric chemistry. *Earth and Planetary Science Letters*, 431: 264-273.
- Kampschulte, A., Bruckschen, P., Strauss, H., 2001. The sulphur isotopic composition of trace sulphates in Carboniferous brachiopods: implications for coeval seawater, correlation with other geochemical cycles and isotope stratigraphy. *Chemical Geology*, 175(1-2): 149-173.
- Kampschulte, A., Strauss, H., 1998. The isotopic composition of trace sulphates in Paleozoic biogenic carbonates: implications for coeval seawater and geochemical cycles. *Min. Mag. A*, 62: 744-745.
- Kampschulte, A., Strauss, H., 2004. The sulfur isotopic evolution of Phanerozoic seawater based on the analysis of structurally substituted sulfate in carbonates. *Chemical Geology*, 204(3-4): 255-286.
- Kaufman, A.J., Knoll, A.H., 1995. Neoproterozoic variations in the C-isotopic composition of seawater: stratigraphic and biogeochemical implications. *Precambrian Res*, 73(1-4): 27-49.
- Lan, Z. et al., 2019. An integrated chemostratigraphic ( $\delta^{13}\text{C}$ - $\delta^{18}\text{O}$ - $^{87}\text{Sr}/^{86}\text{Sr}$ - $\delta^{15}\text{N}$ ) study of the Doushantuo Formation in western Hubei Province, South China. *Precambrian Research*, 320: 232-252.
- Li, C. et al., 2017. Uncovering the spatial heterogeneity of Ediacaran carbon cycling. *Geobiology*, 15(2): 211-224.
- Li, C. et al., 2010. A stratified redox model for the Ediacaran ocean. *Science*, 328(5974): 80-3.
- Lomans, B., Van der Drift, C., Pol, A., Den Camp, H.O., 2002. Microbial cycling of volatile organic sulfur compounds. *Cellular and Molecular Life Sciences CMLS*, 59(4): 575-588.

- Loyd, S.J., Berelson, W.M., Lyons, T.W., Hammond, D.E., Corsetti, F.A., 2012a. Constraining pathways of microbial mediation for carbonate concretions of the Miocene Monterey Formation using carbonate-associated sulfate. *Geochimica et Cosmochimica Acta*, 78: 77-98.
- Loyd, S.J. et al., 2012b. Sustained low marine sulfate concentrations from the Neoproterozoic to the Cambrian: Insights from carbonates of northwestern Mexico and eastern California. *Earth and Planetary Science Letters*, 339: 79-94.
- Lu, M. et al., 2013. The DOUNCE event at the top of the Ediacaran Doushantuo Formation, South China: Broad stratigraphic occurrence and non-diagenetic origin. *Precambrian Research*, 225: 86-109.
- Ma, H. et al., 2021. Sulfur and oxygen isotopic compositions of carbonate associated sulfate (CAS) of Cambrian ribbon rocks: Implications for the constraints on using CAS to reconstruct seawater sulfate sulfur isotopic compositions. *Chemical Geology*, 580.
- Marengo, P.J., Corsetti, F.A., Hammond, D.E., Kaufman, A.J., Bottjer, D.J., 2008a. Oxidation of pyrite during extraction of carbonate associated sulfate. *Chemical Geology*, 247(1-2): 124-132.
- Marengo, P.J., Corsetti, F.A., Kaufman, A.J., Bottjer, D.J., 2008b. Environmental and diagenetic variations in carbonate associated sulfate: An investigation of CAS in the Lower Triassic of the western USA. *Geochimica et Cosmochimica Acta*, 72(6): 1570-1582.
- Markovic, S., Paytan, A., Li, H., Wortmann, U.G., 2016. A revised seawater sulfate oxygen isotope record for the last 4 Myr. *Geochimica et Cosmochimica Acta*, 175: 239-251.
- McFadden, K.A. et al., 2008. Pulsed oxidation and biological evolution in the Ediacaran Doushantuo Formation. *Proc Natl Acad Sci U S A*, 105(9): 3197-202.
- Newton, R.J., Pevitt, E.L., Wignall, P.B., Bottrell, S.H., 2004. Large shifts in the isotopic composition of seawater sulphate across the Permo-Triassic boundary in northern Italy. *Earth and Planetary Science Letters*, 218(3-4): 331-345.
- Ohkouchi, N. et al., 1999. Sulfur isotope records around Livello Bonarelli (northern Apennines, Italy) black shale at the Cenomanian-Turonian boundary. *Geology*, 27(6): 535-538.
- Peng, Y. et al., 2014. Widespread contamination of carbonate-associated sulfate by present-day secondary atmospheric sulfate: Evidence from triple oxygen isotopes. *Geology*, 42(9): 815-818.
- Present, T.M., Paris, G., Burke, A., Fischer, W.W., Adkins, J.F., 2015. Large Carbonate Associated Sulfate isotopic variability between brachiopods, micrite, and other sedimentary components in Late Ordovician strata. *Earth and Planetary Science Letters*, 432: 187-198.
- Rennie, V.C., Turchyn, A.V., 2014. The preservation of  $\delta\text{SSO}434$  and  $\delta\text{OSO}418$  in carbonate-associated sulfate during marine diagenesis: A 25 Myr test case using marine sediments. 395: 13-23.
- Ries, J.B., Fike, D.A., Grotzinger, J.P., Pratt, L.M., Lyons, T.W., 2009. Superheavy pyrite ( $\delta^{34}\text{S}_{\text{pyr}} > \delta^{34}\text{S}_{\text{CAS}}$ ) in the terminal Proterozoic Nama Group, southern Namibia: A consequence of low seawater sulfate at the dawn of animal life. *Geology*, 37(8): 743-746.
- Shen, B. et al., 2011. Carbon, sulfur, and oxygen isotope evidence for a strong depth gradient and oceanic oxidation after the Ediacaran Hankschough glaciation. *Geochimica et Cosmochimica Acta*, 75(5): 1357-1373.
- Shen, B. et al., 2008. Stratification and mixing of a post-glacial Neoproterozoic ocean: evidence from carbon and sulfur isotopes in a cap dolostone from northwest China. *Earth and Planetary Science Letters*, 265(1-2): 209-228.
- Shi, W. et al., 2018. Sulfur isotope evidence for transient marine-shelf oxidation during the Ediacaran Shuram Excursion. *Geology*, 46(3): 267-270.
- Shields, G.A., Strauss, H., Howe, S.S., Siegmund, H., 1999. Sulphur isotope compositions of

- sedimentary phosphorites from the basal Cambrian of China: implications for Neoproterozoic-Cambrian biogeochemical cycling. *Journal of the Geological Society*, 156(5): 943-955.
- Siedenberg, K., Strauss, H., Podlaha, O., van den Boorn, S., 2018. Multiple sulfur isotopes ( $\delta^{34}\text{S}$ ,  $\Delta^{33}\text{S}$ ) of organic sulfur and pyrite from Late Cretaceous to Early Eocene oil shales in Jordan. *Organic Geochemistry*, 125: 29-40.
- Sim, M.S., Bosak, T., Ono, S., 2011. Large sulfur isotope fractionation does not require disproportionation. *Science*, 333(6038): 74-77.
- Staudt, W.J., Schoonen, M.A., 1995. Sulfate incorporation into sedimentary carbonates. ACS Publications.
- Theiling, B.P., Coleman, M., 2015. Refining the extraction methodology of carbonate associated sulfate: Evidence from synthetic and natural carbonate samples. *Chemical Geology*, 411: 36-48.
- Thompson, C.K., Kah, L.C., 2012. Sulfur isotope evidence for widespread euxinia and a fluctuating oxycline in Early to Middle Ordovician greenhouse oceans. *Palaeogeography, Palaeoclimatology, Palaeoecology*, 313: 189-214.
- Tostevin, R. et al., 2017. Constraints on the late Ediacaran sulfur cycle from carbonate associated sulfate. *Precambrian Research*, 290: 113-125.
- Toyama, K., Paytan, A., Sawada, K., Hasegawa, T., 2020. Sulfur isotope ratios in co-occurring barite and carbonate from Eocene sediments: A comparison study. *Chemical Geology*, 535.
- Veizer, J., 1983. Trace elements and isotopes in sedimentary carbonates. 11: 265-300.
- Wang, P. et al., 2019. Large accumulations of  $^{34}\text{S}$ -enriched pyrite in a low-sulfate marine basin: The Sturtian Nanhua Basin, South China. *Precambrian Research*, 335.
- Wei, H., Tang, Z., Qiu, Z., Yan, D., Bai, M., 2020. Formation of large carbonate concretions in black cherts in the Gufeng Formation (Guadalupian) at Enshi, South China. *Geobiology*, 18(1): 14-30.
- Werne, J.P., Lyons, T.W., Hollander, D.J., Formolo, M.J., Sinninghe Damsté, J.S., 2003. Reduced sulfur in euxinic sediments of the Cariaco Basin: sulfur isotope constraints on organic sulfur formation. *Chemical Geology*, 195(1-4): 159-179.
- Wood, R.A. et al., 2015. Dynamic redox conditions control late Ediacaran metazoan ecosystems in the Nama Group, Namibia. *Precambrian Research*, 261: 252-271.
- Wotte, T., Shields-Zhou, G.A., Strauss, H., 2012. Carbonate-associated sulfate: Experimental comparisons of common extraction methods and recommendations toward a standard analytical protocol. *Chemical Geology*, 326-327: 132-144.
- Wotte, T., Strauss, H., Sundberg, F.A., 2011. Carbon and sulfur isotopes from the Cambrian Series 2–Cambrian Series 3 of Laurentia and Siberia. *Museum of Northern Arizona Bulletin*, 67: 43-63.
- Wynn, P.M., Fairchild, I.J., Baker, A., Baldini, J.U.L., McDermott, F., 2008. Isotopic archives of sulphate in speleothems. *Geochimica et Cosmochimica Acta*, 72(10): 2465-2477.
- Xiao, S. et al., 2012. Integrated chemostratigraphy of the Doushantuo Formation at the northern Xiaofenghe section (Yangtze Gorges, South China) and its implication for Ediacaran stratigraphic correlation and ocean redox models. *Precambrian Research*, 192-195: 125-141.
- Zerkle, A.L., Claire, M.W., Domagal-Goldman, S.D., Farquhar, J., Poulton, S.W., 2012. A bistable organic-rich atmosphere on the Neoproterozoic Earth. *Nature Geoscience*, 5(5): 359-363.
- Zhang, X., Zhou, X., Hu, D., 2020. High-resolution paired carbon isotopic records from the Meishucun section in South China: Implications for carbon cycling and environmental changes during the Ediacaran-Cambrian transition. *Precambrian Research*, 337.

## Experimental comparisons of carbonate-associated sulfate extraction methods

Zheyu Tian<sup>a,\*</sup>, Graham A. Shields<sup>a</sup>, Ying Zhou<sup>a</sup>

<sup>a</sup>Department of Earth Sciences, University College London, WC1E 6BS, London, UK, [z.tian.17@ucl.ac.uk](mailto:z.tian.17@ucl.ac.uk)

### Supplementary Information:

Table S1. Elemental concentrations of the acid-soluble fractions of the samples measured by ICP-OES. Carbonate content (%): weight percentages of acid-leachable content (CaCO<sub>3</sub> + MgCO<sub>3</sub>).

Sample	Ca (%)	Mg (ppm)	Al (ppm)	K (ppm)	Fe (ppm)	Mn (ppm)	Sr (ppm)	Mn/Sr	Mg/Ca	Sr/Ca	Fe/Ca	Carbonate content (%)
QLKS18	20.14	122301	154.37	43.42	38.59	155.81	43.42	3.59	0.61	0.00022	0.00019	93.16
QLKS6	36.65	11917.94	47.71	23.85	4.77	32.92	1125.95	0.029	0.033	0.0031	0.000013	95.80
CC3	30.65	8433.85	121.60	325.88	525.29	14.11	3706.23	0.0039	0.028	0.012	0.0017	79.57
LHA6.5	33.97	3398.95	130.19	91.19	1940.90	333.85	207.06	1.61	0.010	0.00061	0.0057	86.11

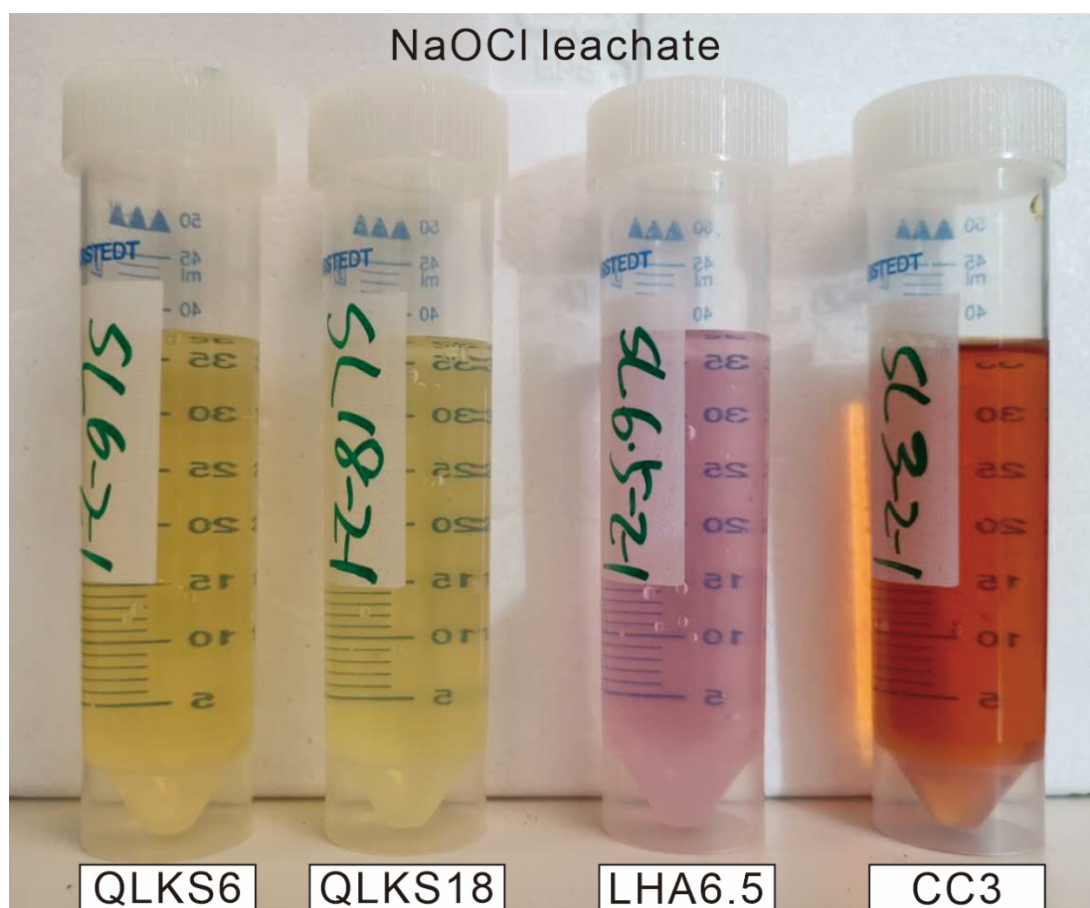


Fig. S1. NaOCl leachate with pink to brown colour showing the pyrite and possibly TOC has been oxidised.

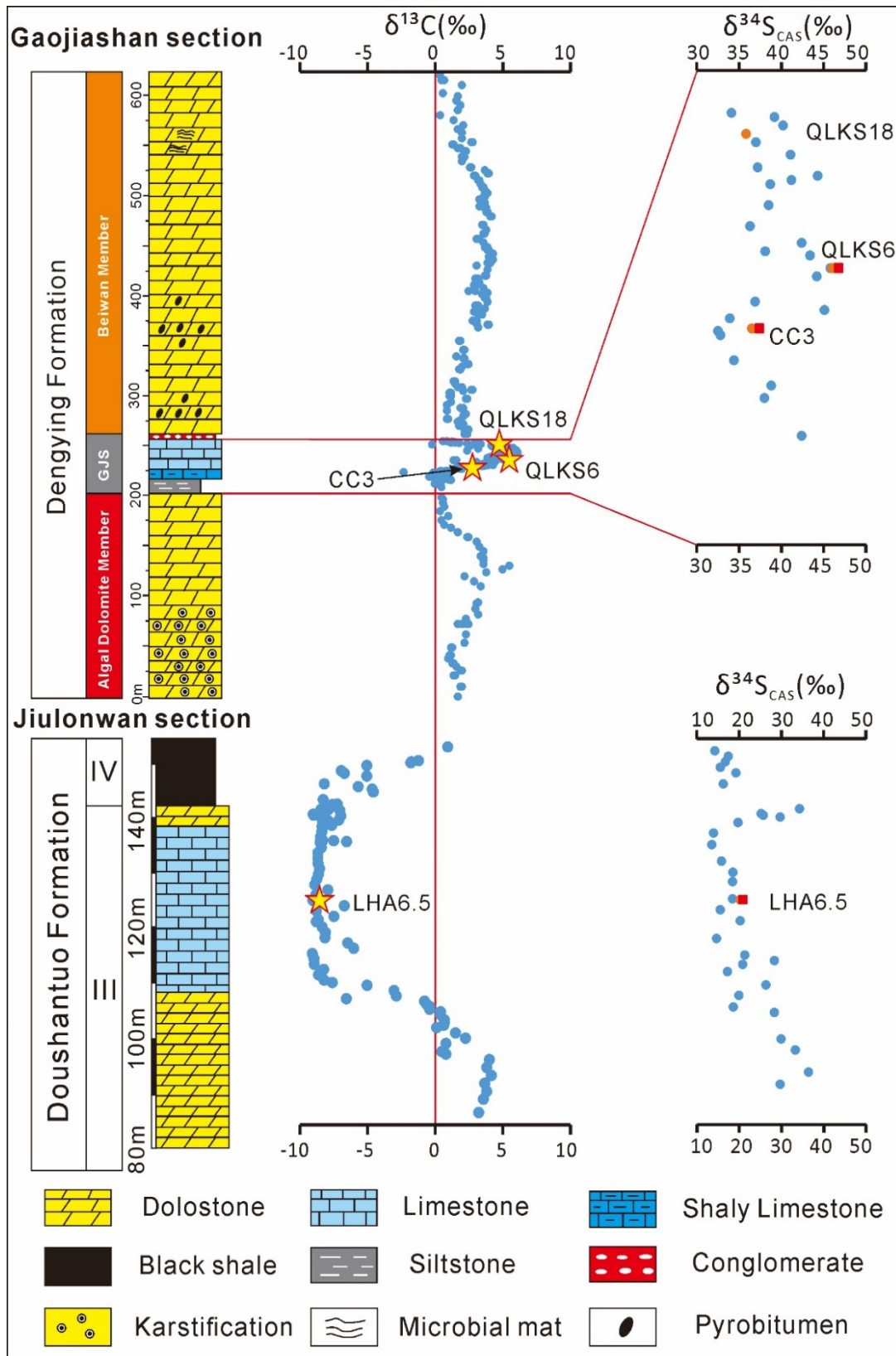


Fig. S2. Comparison of the published  $\delta^{34}\text{S}_{\text{CAS}}$  (‰) and the data from this study using method 1 (orange circles) and method 3 (red square). Sample LHA6.5 is from the Lianghong section. Sample CC3 is from the Zhimaping section. Sample QLKS6 and QLKS18 are from the Qinglinkou section. The blue dots are published data from (Cui et al., 2016; Shi et al., 2018). GJS = Gaojiashan Member.

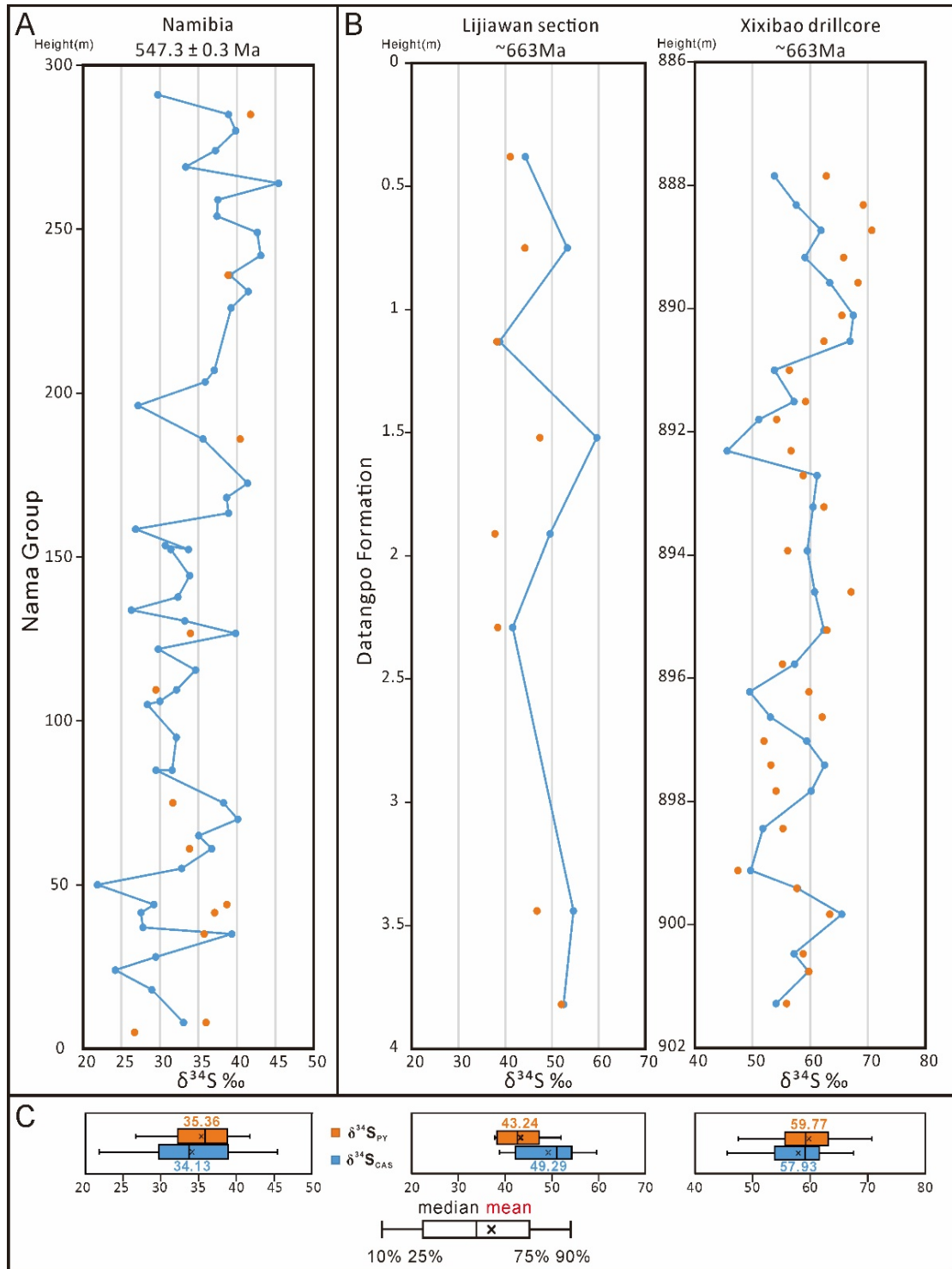


Fig. S3. Comparison of published  $\delta^{34}\text{S}_{\text{CAS}}$  (blue color) and  $\delta^{34}\text{S}_{\text{PY}}$  (orange color) data measured from 'superheavy pyrite' sections. A: Nama Group ( $\sim 547.3 \pm 0.3$  Ma) data from (Tostevin et al., 2017). B: Datangpo Formation ( $662.9 \pm 4.3$  Ma to  $654.5 \pm 3.8$  Ma) data from (Wang et al., 2019a). C: Box plots of corresponding data. The black lines and cross symbols in each box show the median and mean values, respectively.

## Diagenetic Evaluation

Samples with calcium carbonate content >70% and Mg/Ca <0.025 are shown in Fig. S4-A as limestones (LM), calcium carbonate content >70% and Mg/Ca >0.025 are dolomitic limestones (DL) and calcium carbonate content <70% are dolostones (DM). On this basis, Fig. S4-A shows that sample QLKS18 is near stoichiometric dolomite, while the others are limestones.

Cross-plots of Mn/Sr, Mg/Ca, Sr/Ca, and Fe/Ca are commonly used to evaluate the extent of diagenetic alteration, as dissolution and recrystallisation can raise Mn, Fe, and Zn contents and lower Sr, Na contents (Bartley et al., 1998; Kaufman and Knoll, 1995; Lan et al., 2019). Mn/Sr lower than 2, Sr/Ca higher than 0.001, Mg/Ca lower than 0.257 and Fe/Ca lower than 0.01 indicate that the limestone samples in this study have undergone limited diagenetic alteration (Fig. S4). The low CAS yield from sample QLKS18 is perhaps unsurprising due to dolomitisation, which typically occurs under sulphate-reducing conditions (Fichtner et al., 2017; Staudt and Schoonen, 1995; Swart, 2015); however, we note that several published studies report dolomite CAS isotopic data, implying that carbonate-associated sulfate can withstand burial diagenesis and potentially record the paleo seawater  $\delta^{34}\text{S}_{\text{CAS}}$  signature (Fichtner et al., 2017; Guo et al., 2015; Shi et al., 2018; Tostevin et al., 2017). Although we tried several times with sample QLKS18, we failed to get enough  $\text{BaSO}_4$  precipitate for isotopic analysis.

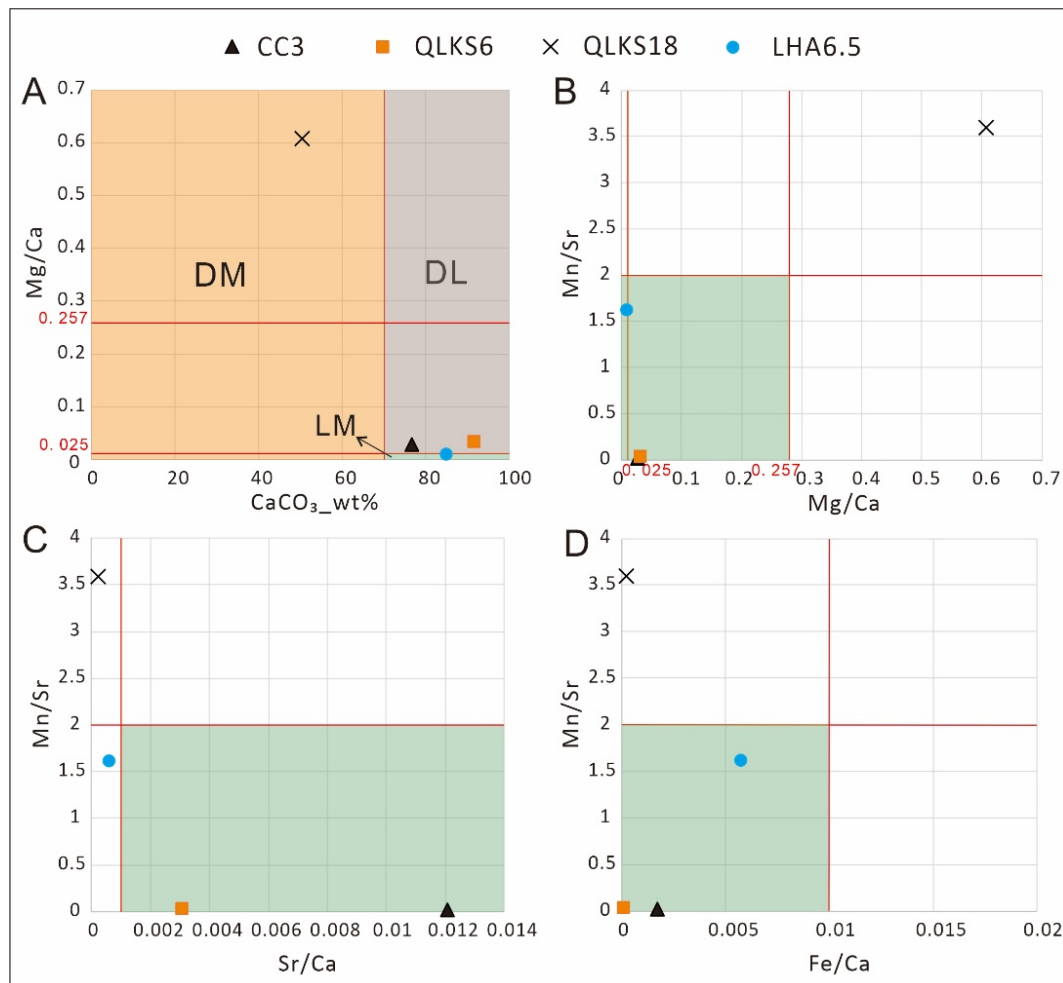


Fig. S4.: Cross-plot of the selected samples. DM: dolomite (calcium carbonate content < 70%); DL: dolomitic limestone (calcium carbonate content >70%; Mg/Ca > 0.025); LM: limestone (calcium carbonate content >70%; Mg/Ca < 0.025). Thresholds for the green shaded area (best-preserved samples) are Mn/Sr < 2, Sr/Ca > 0.001, Mg/Ca < 0.257 and Fe/Ca < 0.01.

### Sample Descriptions

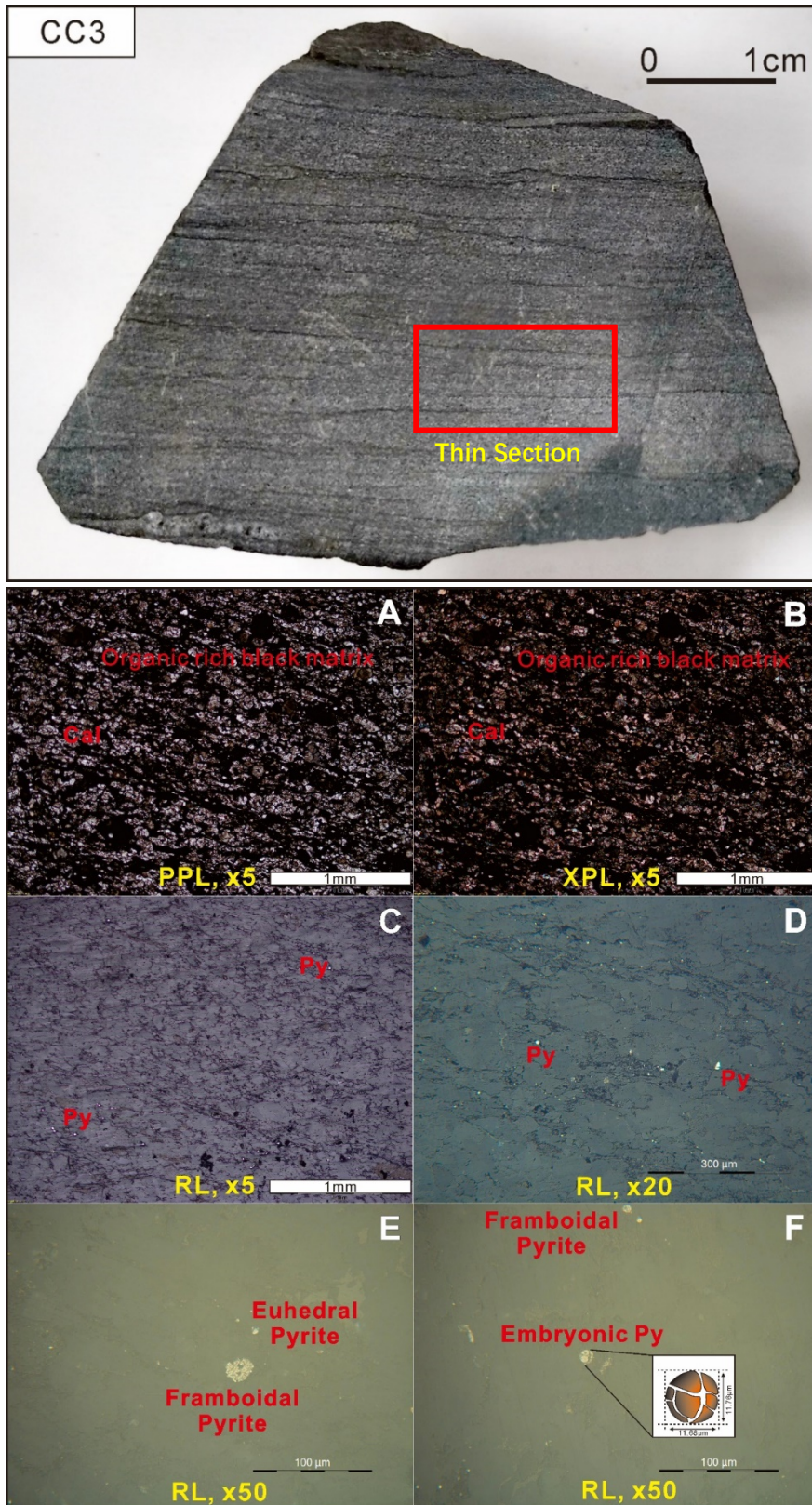


Fig. S5. Sample CC3: Dark thin banded micritic limestone rock rich in organic matter. Microphotographs show the rock is dark grey banded fine-grained limestone (grain size ~0.028mm). A: Sparry calcite grains (PPL, x5). B: Organic-rich black mud matrix (XPL, x5). C: Seminated pyrite (RL, x5). D: Euhedral pyrite (RL, x20). E: Framboidal pyrite (RL, x50). F: Pyrite with the shape of a metazoan (RL, x50). PPL = plane-polarized light; XPL = cross-polarized light; RL: reflected light; Py = pyrite; Cal = Calcite.

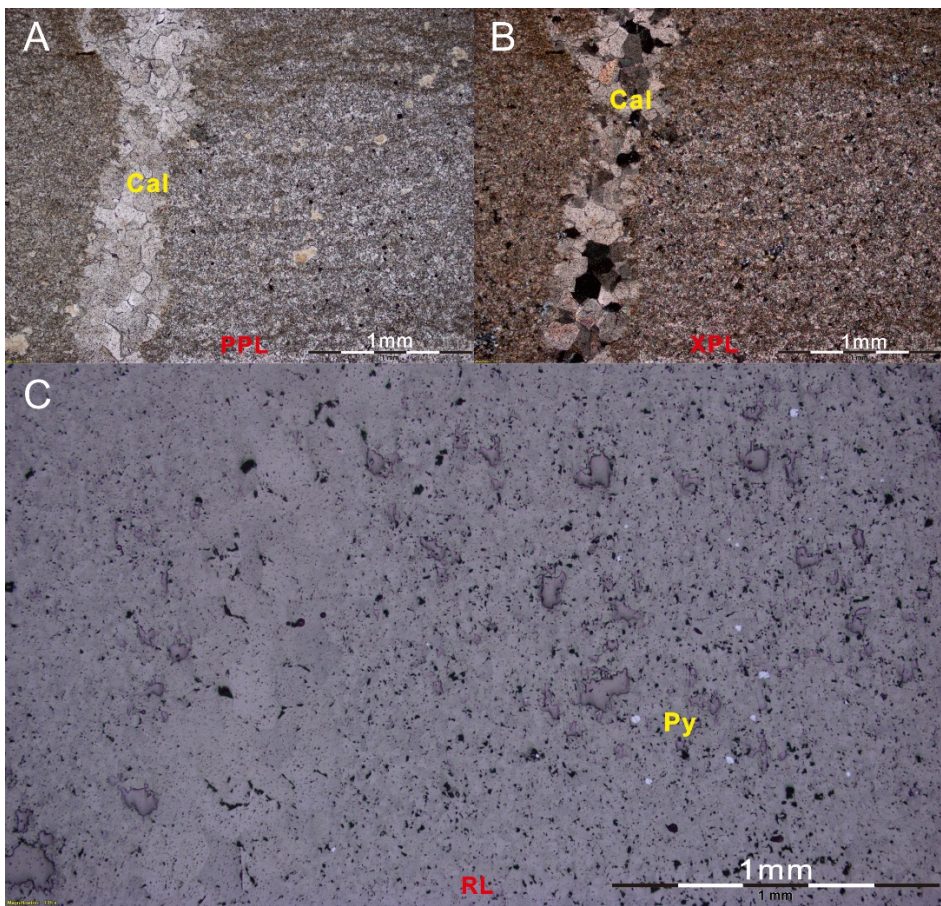
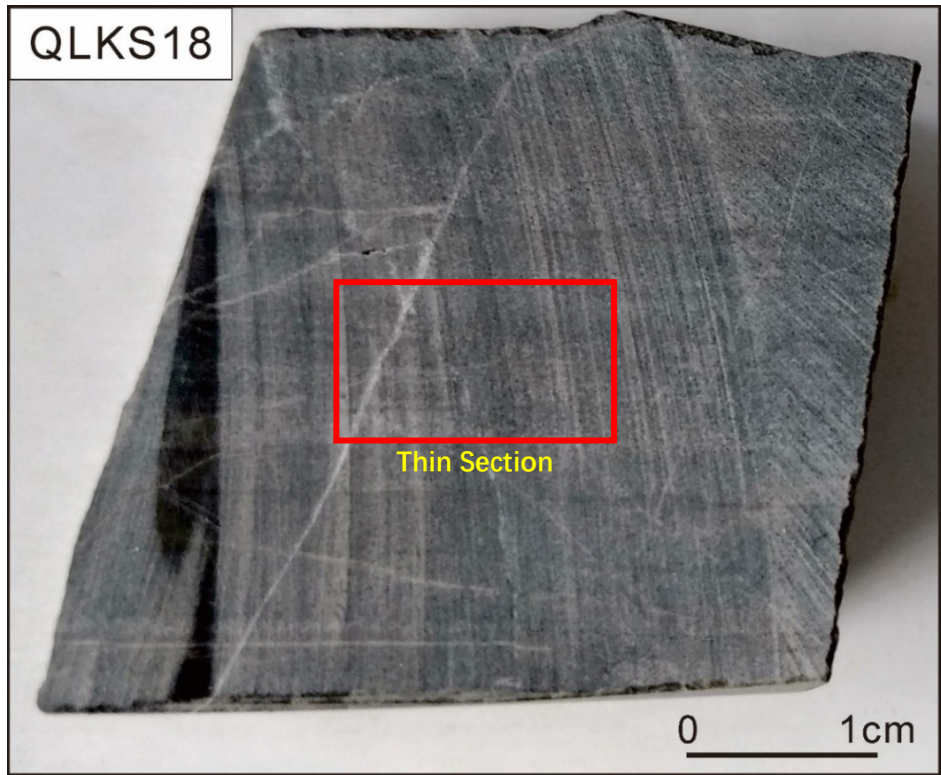


Fig. S6. Sample QLKS18: The rock here is a fine-grained dolomitic limestone rock with some white calcite veins cut through. Photomicrograph shows the rock is limestone (grain size  $\sim 0.019\text{mm}$ ). A: Sparry calcite grains (PPL, x5). B: Calcite dyke cut through the thin section (XPL, x5). C: Seminate euhedral pyrite (RL, x5).

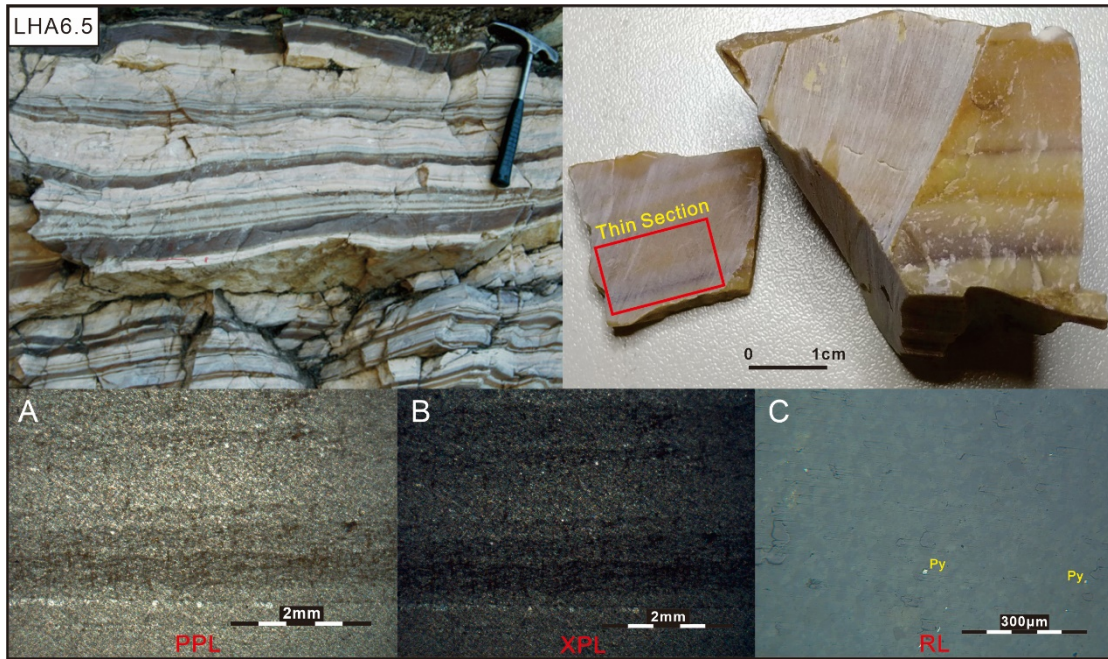


Fig. S7. Sample LHA6.5: The rock here is a grey fine-grained banded limestone (grain size  $\sim 0.022\text{mm}$ ) from Doushantuo member III, Lianghong section, Southern Sichuan. A-B: thin bedded limestone (x2.5). C: euhedral pyrite (RL, x20)

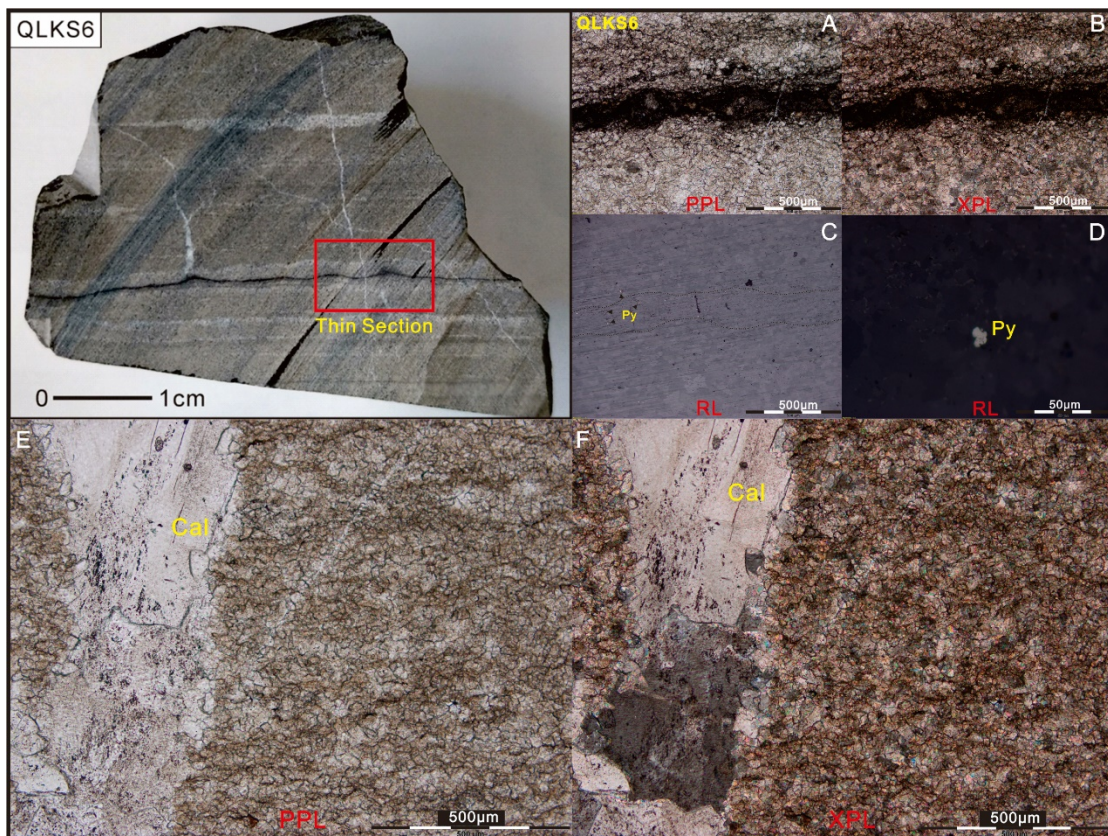


Fig. S8. Sample QLKS6: This sample is dark grey thinly laminated micritic limestone rock (grain size  $\sim 0.027\text{mm}$ ) with white calcite veins cut through. Sample from Shibantan member, Dengying Formation, Qinglinkou Section. Microphotographs show the rock is fine-grained limestone. A-B: Organic rich thin layer interbedded with the carbonate layers (x10). C: Seminate pyrite (RL, x10). D: Framboidal pyrite (RL, x100). E-F: Sparry calcite grains inside the calcite vein (x10).

## References

- Bartley, J.K., Pope, M., Knoll, A.H., Semikhatov, M.A., Petrov, P., 1998. A Vendian-Cambrian boundary succession from the northwestern margin of the Siberian Platform: stratigraphy, palaeontology, chemostratigraphy and correlation. *Geol Mag*, 135(4): 473-94.
- Cui, H. et al., 2016. Environmental context for the terminal Ediacaran biomineralization of animals. *Geobiology*, 14(4): 344-63.
- Fichtner, V. et al., 2017. Diagenesis of carbonate associated sulfate. *Chemical Geology*, 463: 61-75.
- Guo, H. et al., 2015. Sulfur isotope composition of carbonate-associated sulfate from the Mesoproterozoic Jixian Group, North China: Implications for the marine sulfur cycle. *Precambrian Research*, 266: 319-336.
- Kaufman, A.J., Knoll, A.H., 1995. Neoproterozoic variations in the C-isotopic composition of seawater: stratigraphic and biogeochemical implications. *Precambrian Res*, 73(1-4): 27-49.
- Lan, Z. et al., 2019. An integrated chemostratigraphic ( $\delta^{13}\text{C}$ - $\delta^{18}\text{O}$ - $^{87}\text{Sr}/^{86}\text{Sr}$ - $\delta^{15}\text{N}$ ) study of the Doushantuo Formation in western Hubei Province, South China. *Precambrian Research*, 320: 232-252.
- Shi, W. et al., 2018. Sulfur isotope evidence for transient marine-shelf oxidation during the Ediacaran Shuram Excursion. *Geology*, 46(3): 267-270.
- Staudt, W.J., Schoonen, M.A., 1995. Sulfate incorporation into sedimentary carbonates. ACS Publications.
- Swart, P.K., 2015. The geochemistry of carbonate diagenesis: The past, present and future. *Sedimentology*, 62(5): 1233-1304.
- Tostevin, R. et al., 2017. Constraints on the late Ediacaran sulfur cycle from carbonate associated sulfate. *Precambrian Research*, 290: 113-125.
- Wotte, Strauss, Fugmann, Garbe-Schönberg, 2012, *Geochemica et Cosmochemica Acta* 85, 228-253.